Seventh Annual Conference

AMERICAN SOCIETY OF BIOMECHANICS

ABSTRACTS

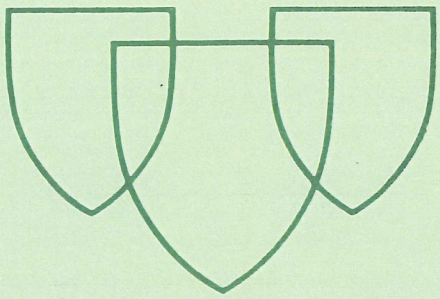

Mayo Clinic
Rochester, Minnesota

September 28-30, 1983

TABLE OF CONTENTS

	Page
Keynote Lectures	1
Session 1A - Ergonomics I	5
Session 1B - Bone Mechanics	9
Session 2A - Orthopaedic Biomechanics I	13
Session 2B - Spine I	17
Session 3A - Soft Tissue	21
Session 3B - Ergonomics II	25
Session 4A - Human Function and Performance	29
Session 4B - Orthopaedic Biomechanics II	32
Session 5A - Locomotion I	35
Session 5B - Spine II	39
Session 6 - Biofluid/Biosolid Mechanics I	43
Session 7A - Locomotion II	46
Session 7B - Biofluid/Biosolid Mechanics II	48

CONFERENCE PROGRAM

Thursday, September 29

8:15 a.m.

Opening, Welcome and Announcements

8:30-9:00

Keynote Lecture: Biomechanical Factors of Chronic Trauma Disorders of the Upper Extremity. T. Armstrong, University of Michigan

9:00-10:20

SESSION 1A ERGONOMICS I
Chairperson: M.H. Pope

9:00

A Biomechanical Model of the Lumbosacral Joint for Lifting Activities. C. Anderson, University of Michigan

9:20

An Evaluation of Handle Shapes and Forces. D. Cochran and M.W. Riley, University of Nebraska

9:40

Measurement of Loads Upon the Lumbar Spine during Isometric and Isokinetic Lifting Activities. W. Marras, R. Joynt and A. King, Ohio State University and Wayne State University

10:00

A Probable Etiology of Mechanical Low Back Pain. J.A. Porterfield, Akron City Hospital

9:00-10:20

SESSION 1B Bone Mechanics
Chairperson: E.Y. Chao

9:00

Fatigue Behavior of Immature Primate Cortical Bone. T.S. Keller, J.D. Lovin, D.M. Spengler and D.R. Carter, VAMC Seattle, University of Washington, University Hospital, Seattle and Stanford University

9:20

A Theoretical Model for Mechanically Induced Bone Remodeling. D.T. Davy and R.T. Hart, Case Western Reserve University and Tulane University

9:40

Surface Strain Studies of the Human Patella. S.A. Goldstein, A.P.C. Weiss, R. Kasman and L.S. Matthews, University of Michigan

10:00

Anaylsis of the Geometric Properties of Human Long Bones Using Computed Axial Tomography, D.L. Dickie, S.A. Goldstein, M.J. Flynn, and P. Bridges, University of Michigan

10:20-10:40

Break

10:40-12:00

SESSION 2A Orthopaedic Biomechanics I
Chairperson: S.A. Goldstein

10:40

Kinematics and Stabilizing Roles of Capsuloligamentous Structures in Index Metacarpophalangeal Joint. A. Minami, Kai-Nan An, W.P. Cooney, R.L. Linscheid and E.Y.S. Chao, Mayo Clinic

11:00

Mathematical Model of the Hip Capsule in Congenital Hip Disease. G.T. Rab, University of California, Davis

11:20

An Analytical Stereophotogrammetric Method to Measure the 3-D Geometry of Articular Surfaces. R. Huiskes and A. de Lange, Univ. of Nijmegen, The Netherlands

11:40

Computer Modelling of Proximal Femur Osteotomies. D.R. Pedersen and R.A. Brand, University of Iowa

10:40-12:00

SESSION 2B Spine I
Chairperson: S. Kumar

10:40

Photogrammetric Measurement of Intervertebral Disc Deformation. I.A.F. Stokes, D.M. Greenapple, University of Vermont

11:00

Compression Studies in the Human Thoracolumbar Spine. A. Sances, D. Maiman, J. Myklebust, S. Larson, J. Cusick, M. Chilbert, R. Jodat, C. Ewing and D. Thomas, Medical College of Wisconsin

11:20

The Effect of Gender on the Strength Characteristics of Squirrel Monkey Vertebral Bodies. S.D. Smith-Lagnese and L.E. Kazarian, Wright-Patterson Air Force Base

11:40

Measurement of Intracompartmental Pressure in the Back. D. Carr, J.W. Frymoyer, L. Gilbertson, M.H. Krag and M.H. Pope, University of Vermont

12:00-1:00

Lunch

1:00-1:50

Instructional Course I
Measurement of *In Vivo* Muscle Forces during Animal Locomotion, Robert Gregor, University of California, Los Angeles

1:50-2:05

Presidential Address

2:05-2:35

Keynote Lecture: Some Progress Toward a Quantitive Description of Human Neuromuscular Dynamics. G.I. Zahalak, Washington University

2:35-3:55

SESSION 3A Soft Tissue
Chairperson: D.T. Davy

2:35

Effect of Immobilization and Remobilization on the Properties of the Medial Collateral Ligaments. S.L.Y. Woo, P.O. Newton and M.A. Gomez, University of California, San Diego

2:55

The Importance of Vascularity and Continuous Motion in Biological Ligament Substitution. D.L. Butler, F.R. Noyes, E.S. Grood, M. Siegel, M.L. Olmstead, R.B. Hohn and R. Kaderly, University of Cincinatti and Ohio State University

3:15

The Functional Relationship between Strain in the Posterior Oblique Fibers and the Parallel Long Fibers of the Human Knee Medial Collateral Ligament. R.A. Fisher, S.W. Arms, M.H. Pope, Robert J. Johnson, University of Vermont

3:35

Surface Strains in Human Patellar Tendon-Bone Units. D.C. Stouffer, D.L. Butler, and R.F. Zernicke, University of Cincinnati and University of California, Los Angeles

2:35-3:55

SESSION 3B Ergonomics II
Chairperson: W. Marras

2:35

A Computerized Three-Dimensional Biomechanical Static Strength Prediction Model for Studying Stresses from Manual Materials Handling Operations. A. Garg and D. Chaffin, University of Wisconsin, Milwaukee and University of Michigan

2:55

Modeling Active Neuromuscular Response to Mechanical Stress. A. Freivalds and I. Kaleps, Pennsylvania State University and Wright Patterson Air Force Base

3:15

Spectral Analysis of Paraspinal EMG Fatigue Characteristics. M.H. Pope, D. Keller, D. Donnermeyer, D. Wilder, University of Vermont

3:35

Construction of a Police Physical Fitness Battery as a Substitute for Age Requirements. R.A. Mostardi, J. Porterfield and S. Urycki, Akron City Hospital

3:55-4:15

Break

4:15-5:15

SESSION 4A Human Performance and Function
Chairperson: K.N. An

4:15

Quantitative Analysis of Forearm Musculature. R.M. Gross, E.Y. Chao and K.N. An, Mayo Clinic

4:35

Mechanical Efficiency of Overarm Throw in Handball. H. Yamamoto and M. Adrian, Washington State University

4:55

Design Analysis of the Biomechanical Ankle Platform System. G.W. Gray, Paramedical Associates Sports Medicine

4:15-5:15

SESSION 4B Orthopaedic Biomechanics II
Chairperson: D.L. Butler

4:15

Fatigue Performance of Hoffman-Vidal External Fixator. R. Shiba, E.Y. Chao, R. Kasman, and M. Cabanela, Mayo Clinic

4:35

An Evaluation of Variables which Alter the Mechanical Behavior of Unilateral Fixator Frames. F. Behrens and W.D. Johnson, St. Paul-Ramsey Medical Center

4:55

Bone Mineral Content in the First Metatarsal: Norms for Women. R.B. Martin and R.A. Yeater, West Virginia University

7:00 p.m.

Dinner, Mayo Foundation House

Friday, September 30

8:30-9:00 a.m.

Keynote Lecture: Locomotion and Posture of the Earliest Human Ancestors. R. Susman, State University of New York at Stony Brook

9:00-10:20

SESSION 5A Locomotion I
Chairperson: J.G. Hay

9:00

Characterization of Joint Moment Patterns as a Function of Walking Speed. S.S. Schein, T.P. Andriacchi and A.B. Strickland, Rush-Presbyterian-St. Lukes Medical Center, Chicago

9:20

Three Dimensional Lower Extremity Joint Forces and Torques in Walking. M. Sabri Eken and M. Donath, University of Minnesota

9:40

An Analysis of Stairclimbing in Anterior Cruciate Deficient Subjects. M.K. Belcher, B. Reider and T.P. Andriacchi, Rush-Presbyterian-St. Lukes, Medical Center, Chicago

10:00

Pattern Recognition Features for Identifying Gait Disability Based on the Angle-Angle Diagram. J. Macfarlane and M. Donath, University of Minnesota

9:00-10:20

SESSION 5B Spine II
Chairperson: I.A.F. Stokes

9:00

In vivo Measurement of Spinal Column Vibrations. M. Panjabi, G. Andersson, L. Jorneus, E. Hult and L. Mattsson, Yale Medical School and Shalgren Hospital, Sweden

9:20

Evaluation of Spinal Deformity by Means of Intrinsic Curvature and Torsion. J. Dansereau, P. Allard, P.S. Thiry, J.V. Raso, and M. Duhaime, Ecole Polytechnique, Montreal, Sainte-Justine Hospital and McGill University

9:40

The Strength of Spinal Ligaments. J.B. Myklebust, F. Pintar, D. Maiman, and A. Sances, Medical College of Wisconsin and Wood V.A. Medical Center

10:00

Analysis of Loads of the Lumbar Trunk during Hammer Throw. I. Hwang and M. Adrian, Yonsei University, Korea and Washington State University

10:20-10:40

Break

10:40-11:10

Keynote Lecture: The Mechanics of Lung Parenchyma. Theodore Wilson, University of Minnesota

11:10-12:10

SESSION 6 Biofluid/Biosolid Mechanics I
Chairperson: E. Grood

11:10

Shearing of Mucus by Cilia as Indicated by Velocity Profiles in Mucocilliary Flows. H. Winet, G.T. Yates, T.Y. Wu and J. Head, California Institute of Technology and University of Southern California Medical School

11:30

Strain Energy Characterization of Human Aortic Tissue in Uniaxial Tension. K.B. Sahay and D. Mohan, Indian Institute of Technology

11:50

Finite Deformation of the Left Ventricle in Isovolumetric Relaxation. S.E. Moskowitz, Hebrew University, Jerusalem

12:10-1:10

Lunch

1:10-2:00

Instructional Course II
Kinetics of Animal Movement. J.G. Andrews, University of Iowa

2:00-2:40

SESSION 7A Locomotion II
Chairperson: T.P. Andriacchi

2:00

A Laser Scanning System for Tracking Motion in 3-D Space for Biomechanical Applications. J.F. Macfarlane and M. Donath, University of Minnesota

2:20

Influence of Passive Elastic Joint Moments on Human Gait. J.M. Mansour and M. Audu, Case Western Reserve University

2:00-2:40

SESSION 7B Biofluid/Biosolid Mechanics II
Chairperson: T. Wilson

2:00

The Sensitivity of Skin to Strain Rate of Loading. Roger C. Haut, General Motors Research Laboratories

2:20

The 20MHz Pulsed Ultrasonic Doppler Velocity Meter: A Method for Assessing Flow in Small Vessels. W.F. Blair and D.R. Pedersen, University of Iowa

2:40-3:20

Business Meeting

BIOMECHANICAL ASPECTS OF CUMULATIVE TRAUMA DISORDERS

by

Thomas J. Armstrong
The University of Michigan
Ann Arbor, MI 48109

Cumulative trauma disorders are a group of musculo-tendinous-osseous-nervous disorders that are caused, precipitated or aggravated by repeated exertions or movements of the body. They are a major concern in industries where 10% to 20% of the people who perform certain manual jobs are affected each year. Control of cumulative trauma disorders has been facilitated by biomechanical modes that can be used to study how stresses are transmitted through the musculo-skeletal system and affect biological tissues. Two types of disorders, tenosynovitis and carpal tunnel syndrome, have been studied most extensively.

Tenosynovitis, an irritation of the tendons and tendon sheaths, often occurs in the wrist where the long tendons of the forearm flexor and extensor muscles slide over and against adjacent boney and ligamentous surfaces. Examplary are the tendons of the flexor digitorum profundus and superficialis tendons inside the carpal tunnel. As the wrist is flexed and extended, the tendons are stretched around the flexor retinaculum and the carpal bones much like a belt around a pulley. The area of maximum stress can be predicted based on the mechanics of a low friction pulley-belt system. Post-mortum studies of the histological character of synovial membrane shows that retrogressive changes in fibrous tissue density, in synovial, subsynovial, and adjacent connective tissue density commonly occur at the site of maximum stress inside the carpal tunnel. Other studies of tendonitis have focused on the viscoelastic properties of tendons. It can be shown that many work activities result in as much as 5% stretching of tendons during a work shift and require several hours for complete recovery. This elongation may distort the vasculature and lead to ischemic tendon damage. In extreme cases tearing of the collagen fibers may occur. Viscoelastic models show great potential for predicting acceptable work-rest schedules for repetitive manual work. DeQuervain's syndrome, tendonitis in the extrinsic abductor and extensor tendons of the thumb at the base of the thumb, is associated with ulnar deviation which stretches the tendons tight over the radial styloid process. It is recommended that jobs be designed so that they can be performed without ulnar or radial deviation of the wrist.

The carpal tunnel also is a common site of median nerve compression. Chronic compression can be caused by swelling of tendons and synovial membranes inside the ligamentous-osseous structure of the carpal tunnel. Post mortum studies show that retrogressive changes including median nerve tissue epineurium density, arteriole wall-muscle thickness, and arterial and venule endoproliferation closely parallel changes of the tendon sheaths. Acute nerve compression between the tendons and the flexor retinaculum can be caused by exertions with a flexed wrist. Exertions with a hyper-extended wrist cause stretching of the median nerve around the carpal bones. It is recommended that jobs be designed so that they can be performed without flexion or hyper-extension of the wrist.

SOME PROGRESS TOWARD A QUANTITATIVE DESCRIPTION OF HUMAN NEUROMUSCULAR DYNAMICS

KEY - 2

George I. Zahalak
Department of Mechanical Engineering Washington University St. Louis MO 63130

The importance of a quantitative description of the dynamic behavior of human skeletal muscle as it functions normally in-vivo hardly needs to be stressed. The *magnitudes* of muscular stiffness, contraction time constants, and reflex feedback intensity (to list a few of the most important parameters) have a critical bearing on many problems in Biomechanics, ranging from the theoretical (eg. the mechanism of physiological tremor) to the practical (eg. the design of limb prostheses). Equally, it needs hardly be stressed to workers in the field that such a quantitative description is very difficult to obtain. The mechanical behavior of a muscle depends on its history of neural activation, and the only relatively accessible measure of neural activation is the surface electromyogram (EMG). Unfortunately the EMG is a rather noisy measure of neural activity, but there do not seem to be many alternatives to its use if one wishes to understand the dynamic response of muscle under general time-varying conditions.

The literature on in-vivo relations between the mechanical variables, -force and length, and the EMG is extensive, but the results are not. The three most commonly used experimental paradigms are static (isometric), constant velocity ("isotonic"), and small-amplitude oscillation tests. I would like to focus in this talk on the third kind of test, - frequency-response tests involving small fractional changes in muscle length, which have yielded considerable information on both muscle mechanics and reflex feedback. In our experiments the relations between the muscle forces contributing to flexion/extension of the forearm about the elbow, the forearm position, and the EMG's from the accessible contributing muscles are examined under two conditions: voluntary oscillations and forced oscillations. The results have suggested a minimal adequate model for the muscle "actuator" as a quasi-linear, second-order, two-input (EMG, length), one-output (force) system. By comparing the behavior of this model to that observed experimentally in the frequency-response tests via a least-squares identification algorithm, numerical estimates have been obtained for the values of the model parameters which characterize normal, adult male subjects. These parameters include muscular stiffness and time constants associated with contraction dynamics. Further, the forced oscillation tests have suggested a model for the reflex feedback arising from small perturbations of the limb. According to this model the reflex EMG arriving at the muscle at a given time is proportional to the muscle stretch, stretch velocity, and stretch acceleration a neural transport time delay previously, except that this feedback signal has passed through an amplitude-limiting saturator. The talk will also describe our new, versatile testing apparatus (the PLTS), and some ongoing experiments designed to verify and extend the results discussed above.

Finally, I would like to discuss the prospects for formulating mathematical models appropriate to describing the dynamics of whole muscle when the fractional changes in muscle length are not small. The classic A.V. Hill model has been used ubiquitously, *faute de mieux*. But there are some well-known (and some not so well-known) problems with this model. I will describe an alternative approach to muscle modelling, termed the Distribution-Moment (D-M) model which I proposed two years ago. This model replaces the single first-order ordinary differential equation of the Hill model by three such equations, but in return it offers a number of advantages including (1) a direct, albeit approximate, connection with current biophysical theories of molecular contraction dynamics, (2) realistic mechanical response in stretch as well as shortening, and (3) simultaneous prediction of stress, strainrate, and chemical energy rates.

Randall L. Susman
Department of Anatomical Sciences
School of Medicine
State University of New York
at Stony Brook
Long Island, New York 11794

ABSTRACT

"The Locomotor and Posture of the Earliest Human Ancestors"

Numerous traits in the postcranial skeleton of the earliest humans (hominids) from Hadar in Ethiopia which lived some 3.5 million years ago provide convincing evidence that terrestrial bipedality was a major component of their terrestrial locomotor behavior. Comparative morphological and experimental analyses of the fossils and living primates reveals a large and interrelated group of features of the hands, feet, and shoulder and suggests that a significant degree of arboreal behavior also constituted the behavioral profile of Hadar hominids. Limb proportions of these hominids and footprints uncovered at Laetoli in Tanzania further suggest a gait for these individuals that differed from that seen in later hominids and living humans. The hand possesses a rod-like pisiform, a small trapezium and small slender thumb, a constricted capitate, long and curved proximal and middle phalanges, and a relatively narrow tufted distal phalanx. All of these traits place the Hadar hominids morphologically between living apes and later hominids. The phalangeal curvatures, and decidedly arboreal aspect, equal or exceed those in living apes. The foot displays a bipedal capacity in the load bearing aspect of the calcaneus and talus, but the toes evidence the functional retention of a strong grasping capability. The shoulder joint is ape-like in its cranial orientation. Finally, the intermembral proportions of the limbs are intermediate between chimpanzees and later hominids. The Hadar hominids possessed a lower limb that was 30% shorter than those in modern humans when scaled for body weight. With a long foot and short overall lower limb the swing phase of walking would have been kinematically different from modern humans.

Two million years later the next grade in human evolution is represented by Homo habilis, the first member of our genus. Homo habilis reveals a mode of bipedalism far advanced over that of the Hadar hominid. The leg and foot of H. habilis display a distinctively human-like, arched, stable plantigrade foot with extrinsic flexors, extensors and pronators similar to those in humans. The hand, however, reveals a primitive climbing ability. Although both the Hadar hominids and later Homo habilis combined terrestrial bipedalism and arboreal climbing in their locomotor repertoires, by 1.76 m.y.B.P. Homo habilis evinces a far smaller component or arborealism than the earlier forms.

The Mechanics of Lung Parenchyma

Theodore A. Wilson, Department of Aerospace Engineering and Mechanics
University of Minnesota, Minneapolis, Minnesota 55455

Lung parenchyma is a foam-like material with a surface area of the order of 400 cm^2/cm^3. It is not surprising, therefore, that the recoil pressure of an air-filled lung is several cm H_2O greater than the recoil pressure of a saline-filled lung, and that surface tension significantly affects the mechanical behavior of the lung. In the past, it has been assumed that the recoil pressure of the air-filled lung could be pictured as simply the sum of the surface tension and tissue contributions and that the tissue contribution is the recoil of the saline-filled lung. Recent data show that surface area is smaller in the air-filled lung than in the saline-filled lung. Apparently, surface tension distorts lung tissue and decreases surface area. Tissue distortion implies tissue forces that also contribute to the recoil pressure of the air-filled lung. By using the idea that, at equilibrium, the total energy (the sum of surface and tissue energies) is minimum, the contributions of surface tension and tissue forces to lung recoil can be sorted out.

In a detailed model for the mechanical structure of lung parenchyma, the tissue elements that contribute each component of recoil pressure are identified. The peripheral tissue system, consisting of the pleural membrane and its extensions that penetrate centripitally into the lung, provides the recoil of the saline-filled lung. Punch indentation tests show that the pleural membrane constitutes a surprisingly large fraction, nearly half, of this component. Helical fibers that form the free edges of the alveolar walls bordering the alveolar duct provide the additional tissue component of recoil in the air-filled lung. The inward component of the hoop force that results from the tension in these curved line elements balances the outward pull of surface tension. As the duct expands, alveolar wall material folds into the interior corners of the alveoli, and surface area is reduced.

A BIOMECHANICAL MODEL OF THE LUMBOSACRAL JOINT FOR LIFTING ACTIVITIES

by Charles K. Anderson

Damage to ligaments, muscles and the disc at the lumbosacral joint have all been implicated as potential sources of low-back pain. Given the difficulty of examining these deep-lying structures in-vivo, little progress has been made towards understanding the response and limitations of these tissues to different common physical activities which are clinically reported to produce low-back pain. In order to study the responses of these complex tissues, a computerized biomechanical model was developed. The resulting model allows one to estimate the stress and strain in each of the above-mentioned tissues for sagittal-plane two-handed lifting tasks.

The model contains three components, namely;

1) a vertebral re-orientation kinematic model,
2) a flexible-endplate intervertebral disc model, and
3) a ligament/muscle kinetic model.

These specific models were combined into a general biomechanical model of the low-back, which was then evaluated by both sensitivity analyses and comparison with data of other investigators.

The evaluation of the model on simulated lifting activities suggested that typical lifting tasks can lead to excessive disc compressive forces, muscle moment generation requirements, and possibly lumbodorsal fascia strains. On the other hand, annulus rupture due directly to strain on the tissue appears unlikely unless disc degeneration has taken place possibly from earlier endplate fracture, of which there is a relatively high risk. Also, strains on ligaments other than the lumbodorsal fascia are very low relative to levels thought to cause micro-damage for each respective ligament.

In a review of jobs requiring repeated load lifting, high values of lumbodorsal strain, disc compression and muscle force required for trunk extension were all found to be associated with higher incidence rates of low back pain.

AN EVALUATION OF HANDLE SHAPES AND FORCES

David J. Cochran
and
Michael W. Riley

The biomechanical forces exerted by the hand in grasping a handle are complex. Because of the extreme complexity of the human hand and the vast differences in anthropometric measurements and strengths of individual hands, strict biomechanical modeling of grasp, as it is affected by the item to be grasped, is as yet infeasible. This research attempts to evaluate empirically the effects of handle shape on the hand's ability to resist or exert force in six directions. Thirty-six handles of four sizes and nine shapes were tested for maximum force exertion by both males and females. The results showed that different handle shapes and sizes were associated with high and low forces for each of the six directions. This suggests that handles which are associated with high forces on one of the six directional tests are probably suited for tasks which incorporate that type of force or movement and may not be appropriate for other tasks which do not.

MEASUREMENTS OF LOADS UPON THE LUMBAR SPINE DURING ISOMETRIC AND ISOKINETIC LIFTING ACTIVITIES

W. S. Marras
Ohio State University
Columbus, OH 43210

R. L. Joynt
A. I. King
Wayne State University
Detroit, MI 48202

The objective of this study was to investigate the effects of controlled lifting movements upon the spinal musculature and intra-abdominal pressure. Ten male and ten female subjects were tested for their ability to exert maximal force about the lumbo-sacral junction under controlled isometric and isokinetic conditions. A Cybex II dynamometer was used to measure torque under controlled velocity conditions and trunk flexion angles. The pelvis was tightly held by straps to a metal frame. Fine wire electrodes were used to measure EMG activity of ten trunk muscles. Intra-abdominal pressure (IAP) and torque produced by the back were also monitored. The results indicated that there were prominent differences in the utilization of trunk musculature for the production of torque statically and dynamically. The force produced by the latissimus dorsi increased as a function of the trunk flexion angle isokinetically but was not a monotonic function of angle isometrically. Isokinetically, the erector spinae muscle force also increased as a function of trunk angle but only between the erect position and 22.5 deg. It was steady between the angles of 22.5 and 45 deg. Isometrically, it decreased as a function of angle. The erector spinae is the only muscle group which produced a greater force under many isokinetic conditions than under isometric conditions at 45 deg. A significant time delay was identified between the onset of IAP and torque and this lag also increased with increasing trunk velocity. Significant positive correlations were found between IAP and the activity of the latissimus dorsi while there was a lack of correlation between IAP and the activity of the rectus abdominis. These results suggest that isokinetic trunk testing can provide a more effective means of evaluating manual materials handling tasks.

A PROBABLE ETIOLOGY OF MECHANICAL LOW BACK PAIN

James A. Porterfield, L.P.T./A.T.,C./M.A.
Director Physical Fitness Testing Center
Akron City Hospital
525 E. Market St.
Akron, OH 44309

Abnormal asymmetrical antigravity biomechanics often accompanies musculoskeletal symptomatology. Asymmetrical skeletal dimensions couples with the decreased stabilizing affect of our musculature as we age, alters the way in which our contractile and noncontractile soft tissues bear weight. Those with poor antigravity biomechanics render their musculoskeletal system vulnerable to increased wear pattern which often translates to symptom. In effect, people with asymmetrical biomechanics most often lose the battle against gravitational forces sooner than those who are musculoskeletally summetrical.

Our lumbopelvic region is the hub of our weight bearing posture. It is here that the forces from our trunk meet the forces from the ground. In an erect position, our center of gravity lies anterior to the second sacral vertebrae. There is no other area in our body that is more vulnerable to excessive forces than L_4, L_5, and pelvic region. If these forces reach the hub of weight bearing symmetrically, the weight line or the way in which we bear weight is equal bilaterally. However, if, for example, one has a one-half inch structural leg length difference on the right, which is not uncommon in our population, a series of adaptive changes takes place in an attempt to assure stability of the weight line. For example, the lumbar spine (trunk) leans to the left (left side bending) which has an accompanying rotatory force in the opposite direction (Fryette's Law). Therefore, the manner in which gravitational forces are transferred through this region is altered. This series of adaptive changes that begin at the foot and work up (ground forces) as well as those forces that begin at head and move caudal (trunk forces), render the tissue about our center of gravity (all lumbopelvic stabilizers) vulnerable to excessive forces which often exceed their supporting capabilities, and minute tearing or destruction begins.

The role of the clinician is to be aware of such biomechanical changes, diagnosis the total condition properly, assist the individual in normalizing his antigravity biomechanics (posture) and maintaining the dynamic stabilizing qualities of the musculature that unfortunately diminish with age.

FATIGUE BEHAVIOR OF IMMATURE PRIMATE CORTICAL BONE.

Keller, T.S.*; Lovin, J.D.**; Spengler, D.M.***; and Carter, D.R.****

Bone fatigue fracture in vivo is a complex process in which mechanical damage accumulates faster than it can be repaired by normal biological repair (remodeling) processes. In vitro fatigue testing eliminates the interactions between mechanical damage and bone repair, simplifying subsequent analysis. Previous fatigue investigations have examined the behavior of mature compact bone, but no information has been obtained for immature bone. This investigation examines the strain controlled fatigue behavior of immature primate cortical bone, comparing bone obtained from anatomically different regions within the same bone. Monotonic tensile tests to failure were also performed for comparison with fatigue data, and ash weights and densities for each specimen were obtained.

The femora of Papio Cyanocephali Anubis (PCA) primates ranging from 2.3-13.7 years were excised from attaching muscles. A diamond saw was used to cut the femora at mid-diaphysis and at 37mm distal and proximal to mid-diaphysis, effectively dividing the bone into patellar and acetabular cylindrical sections. The cylinders were then sectioned into anterior, posterior, medial and lateral slabs measuring approximately 3x3x37mm. Each slab was machined into a cylindrical specimen having a 10mm gauge length central waisted section, 1.5mm in diameter. Care was taken during sectioning and machining to keep the specimens moistened with Ringer's Lactate. An extensometer was attached to the waisted section enabling strain to be controlled and measured during testing. Thirty-nine specimens were tested in fully reversed axial tension-compression cyclic loading and 10 specimens were subjected to monotonic tensile tests to failure. Stress vs. time, strain vs. time, and stress vs. strain histories were monitored. All tests were performed at 37°C and 100% humidity. A constant strain range of 0.006 and constant strain rate of $0.02sec^{-1}$ were used, resulting in a physiological loading rate of approximately 1.7 HZ. Fatigue failure was defined as either complete fracture or the point at which the stress range fell below 70% of the stress range on the first loading cycle, depending upon which occurred first. Following mechanical testing, dry density and % ash determinations were performed for each specimen.

The fatigue specimens exhibited a gradual, progressive decrease in stress amplitude and an increase in stress/strain hysteresis prior to failure. These changes occurred during the tensile phase of the loading cycle indicating that bone fatigue damage accumulated during the tensile phase of the loading cycle. SEM photomicrographs of the fracture site of failed specimens revealed numerous microcracks extending between lacunae, debonding of interlamellar cement bands, and osteonal pullout characteristic of a tensile mode of failure (matrix damage). The axial modulus, measured during the first loading cycle, increased (10 GPa to 18 GPa) with increasing animal age up to maturity (6 years). The collective moduli of the patellar sections were found to be greater than the acetabular sections (E_{Pat}/E_{Acet} = 1.10) with the Ant.>Post.>Lat.>Med. sections. Bone fatigue resistance, measured as cycles to failure, decreased with increasing age in the range 50,000 cycles-1100 cycles. The patellar sections were found to be more fatigue resistant than the acetabular sections, with fatigue resistance of the Ant.>Post.>Lat.>Med. section. No significant correlations between % ash vs. age and density vs. age were found, the former ranging from 62 to 70% and the latter ranging from 1.4 to 2.0 g/cm^3. Good correlation, however, between modulus and bone ash % and density, and between fatigue resistance and bone ash % and density were found (increasing for increasing % ash and density). In addition, the ultimate stress and strain of the patellar sections were found to be significantly greater than the acetabular sections.

Immature bone exhibits fatigue characteristics similar to those reported for mature bone; age-related variables influence the ultimate fatigue characteristics of bone in vitro. Furthermore, anatomical regions within a particular bone section show marked differences in modulus and fatigue--an adaptive response of bone to varying stress fields and the stresses generated by muscle insertion sites. Thus, the vasti intermedius and lateralis muscles, which originate on the anterior portion of the femur, impart considerable stress to the patellar-anterior portion of the femur in contrast to the medial aspect of the femur, which has no major origins or insertions of muscles. These regions show marked differences in fatigue and material properties. Muscle weaknesses or imbalances may therefore play an important role in the fatigue response of a given anatomical region of immature bone.

*VAMC, Orthopaedic Research Lab, Seattle, WA 98108; **Univ. of Washington, School of Medicine, Seattle, WA 98195; ***Univ. Hospital, Dept. of Orthopaedics, Seattle, WA 98195; ****Mech. Engr. Design Div., Stanford Univ., Stanford, CA 94305.

A THEORETICAL MODEL FOR MECHANICALLY INDUCED BONE REMODELING

D.T. Davy* and R.T. Hart**

A unified modeling concept is presented for relating the remodeling response of bone to the local strain history. The purposes of the model are to more effectively accommodate a number of experimental results which have been reported and to provide a vehicle for more detailed descriptions of the relationships between mechanical and biological parameters in remodeling.

The model is based on the assumption that mechanically induced bone remodeling is the manifestation of cellular activity on local bone surfaces, i.e. the net result of average osteoblastic and osteoclastic activity per unit surface area in the region (1). Both internal and external remodeling is then describable in terms of local surface velocity (2). The relationship between strain history and remodeling activity is regarded as a feedback control loop with external load history as an input. If the material is regarded as elastic, instantaneous local strain is then a consequence of the instantaneous loads, and current geometric and material properties. The local strain history is then assumed to elicit a strain remodeling signal which is modulated by genetic and metabolic factors. The net result is a remodeling potential which determines the average local rate of recruitment and activation of osteoblasts and osteoclasts (2). To complete the feedback loop, the net remodeling which is the sum of the osteogenesis (formation) and osteoclasis (resorption), then determines the current rate at which geometric properties and material properties are changing.

The functional forms of the relationships connecting the various nodes in the control loop are assumed to be time dependent. Specifically, the strain remodeling signal is assumed to be a function of the strain history, and the cellular recruitment rate and activity levels are assumed to be functions of the remodeling potential history. In terms of time histories, the simplest possible relationships would be algebraic relationships between current states of the variables. This assumption leads directly to adaptive elasticity models previously proposed by others (3). In the present study more general relationships, in terms of differential equations relating various control loop parameters have been considered. These lead to models which appear to more adequately describe phenomena such as strain rate effects on remodeling response which have been reported in experimental work by others (4).

(1) Frost, H.L., Bone Dynamics in Osteoporosis and Osteomalacia, Charles C. Thomas Pub. (1966); (2) Martin, B.R., J. Biomech., 5: 447 (1972); (3) Cowin, S.C., in Mech. Prop. of Bone, ASME, p. 193 (1981); (4) O'Connor, J.A., Lanyon, L.E., Trans. ORS, 7: 103 (1982).

*Department of Mechanical and Aerospace Engineering, Case Western Reserve University, Cleveland, OH 44118

**Department of Biomedical Engineering, Tulane University, New Orleans, LA 70115

SURFACE STRAIN STUDIES OF THE HUMAN PATELLA

S.A. Goldstein, Ph.D., A.-P.C. Weiss, B.S.,
R. Kasman, M.S., and L.S. Matthews, M.D.

The Biomechanics, Trauma and Sports Medicine Laboratory
University of Michigan Medical Center
Ann Arbor, Michigan 48109

In order to better understand the function of the normal and polyethylene resurfaced patella, to provide insight into patellar fracture mechanics and treatment, and to provide some experimental data for comparison with finite element analysis predictions, this study of patellar surface strains was performed.

A custom loading frame mounted in an Instron testing machine allowed us to stabilize and adjust seventeen fresh frozen intact cadaver knee joints at flexion positions from 0 to 90 degrees in 15 degree increments. The quadriceps aponeurosis was clamped and attached to the tension load cell and the specimen's position adjusted to approximate the normal direction of the resultant quadriceps force. Experimental quadriceps forces of up to 1800 Newtons were possible.

The bone was carefully prepared and strain gages were attached to upper, middle and lower positions on the superficial surface using cyanoacrylate cement.

Strain recordings were made with the knees flexed at 0 to 90 degrees in 15 degree increments, at loads from 0 to 180 Kg.

After testing, all knees were removed from the loading fixture and a total knee arthroplasty with patellar replacement was performed using either a domed patella with one fixation post or a "total contact" patella with two pegs at proximal and distal locations. The knees were then repositioned in the fixture and testing was repeated.

Seven knees were instrumented with 60 degree rosette strain gages and calculations of principal strains and principal strain directions were performed. The other ten knees were instrumented with single longitudinal gages.

1). Patellar surface strains as high as 1100 microstrain were recorded in the distal gages at a quadricipes force of 1764 Newtons.
2) The highest strains were recorded near the distal pole of the patella which correlates well with clinical fracture experience.
3). The resolved principal strain directions were nearly vertical (0 to 7 degrees).
4) Maximum strain occurs with the knee in 45 to 60 degrees of flexion.
5). Polyethylene prosthetic surface replacement of the patella causes increases in recorded strains of the patella at knee flexion angles greater than 30 degrees. The single central post patella prosthesis caused a greater increases in strain than the double posted total contact patella.

ANALYSIS OF THE GEOMETRIC PROPERTIES OF HUMAN LONG BONES USING COMPUTED AXIAL TOMOGRAPHY

D.L. Dickie, M.S.,* S.A. Goldstein, Ph.D.,*
M.J. Flynn, Ph.D.,** and P. Bridges, M.S.***

*The Biomechanics, Trauma and Sports Medicine Laboratory
(Section of Orthopaedic Surgery)
**Department of Radiology and ***Department of Anthropology
University of Michigan Medical Center

The study of the strength of bone as the human form has evolved has been of interest in the field of biomechanics for decades. The spatial distribution of bone material can provide much information regarding bone function. Due to the value of many fossils, some bones cannot be physically altered (i.e., sectioned) in order to examine material distribution characteristics. The application of computed tomography provides a nondestructive modality with sufficient resolution to accurately determine the geometric properties of bone.

Samples of two ancient Indian populations have been analyzed to compare the effects of pre and post agricultural lifestyles of bone's geometric properties. These properties have been computed directly from the digital CT output data.

The data from a GE 8800 scanner was stored on magnetic tape and transferred into a PDP 11/70 image processing computer system. Using bone phantoms of variable densities, algorithms to minimize boundary detection and threshold errors were written and evaluated.

Cross sectional area, centroid, maximum and minimum fiber length, moments of inertia, relative torsional stiffness and relative bending stiffness were determined for all cross sections.

The system proved to be within the limits of error reported by other investigators using indirect digitization techniques. In addition, the system enables the determination of geometric properties nondestructively and can also be utilized for living patients.

KINEMATICS AND STABILIZING ROLES OF CAPSULOLIGAMENTOUS STRUCTURES IN INDEX METACARPOPHALANGEAL JOINT

Akio Minami, M.D., Kai-Nan An, Ph.D., William P. Cooney III, M.D.
Ronald L. Linscheid, M.D., Edmund Y.S. Chao, Ph.D.

The metacarpophalangeal (MCP) joint, particularly of the index finger, is susceptible to injury through dislocation, subluxation and fracture. Joint stability to restrain isometric pinch and grasp forces is provided by the joint articular surfaces, capsuloligamentous structures and musculotendinous units. The joint ligaments and capsule provide initial stability to instantaneous forces and moments and provide a second-line defense in maintaining stability during static loading conditions. Knowledge of the kinematics and stabilizing roles of the capsuloligamentous structures in the index MCP joint provides useful information for ligament reconstructive surgery and for designing implants.

Gross examination and quantitative measurement of the collateral ligaments (CL) of the index MCP joint were carried out using human cadavers. Anatomically, the CL's appeared to be separated into two layers, one superficial and the other deep. Quantitatively, the distances between origin and insertion of the CL's were studied with biplanar x-ray techniques. When the MCP joint was flexed from 0 to 80 degrees, the dorsal portions of both the radial collateral ligament (RCL) and ulnar collateral ligament (UCL) were significantly lengthened (3 to 4 mm). On the other hand, the volar portions of the ligaments were shortened (1 to 2 mm). In the positions of extension and hyperextension, the dorsal portions of the ligaments shortened 2 to 3 mm, but the volar portions of the ligaments lengthened.

Next, the absolute and relative contribution of the CL's, accessory collateral ligament (ACL), volar plate (VP) and dorsal capsule (DC) around the index MCP joint to stability were studied using an MTS machine. Four types of movement (distraction, pronation-supination, dorsal-volar displacement, abduction-adduction) were tested at both 0 and 75 degrees of flexion.

Results obtained from this study are as follows: 1) Based on capsuloligamentous constraints, the index MCP joint has three degrees of freedom. 2) In distraction and dorsal-volar displacement, the RCL and UCL play major stabilizing roles. 3) The UCL is stiffer than the RCL. 4) The RCL contributes to constraint of pronation and adduction, while the UCL mainly contributes to constraint of supination and abduction. 5) The ACL constrains abduction-adduction to a much lesser extent. 6) The VP contributes only to constraint of dorsal displacement. 7) The DC did not play a significant stabilizing role in any motion.

Mathematical Model of the Hip Capsule in Congenital Hip Disease

George T. Rab, M.D.
Department of Orthopaedic Surgery
University of California, Davis

ABSTRACT

A three-dimensional mathematical model of the hip capsule has been devised. It consists of a series of discreet linear elements of variable stiffness, oriented along lines of longitudinal capsular fibers. The model also includes normal bony anatomy of the acetabulum and proximal femur. The proximal femur is free to rotate in three dimensions, allowing study of the effect of femoral position on capsular tightness and interarticular stability.

The model has been used to investigate various factors of stability in congenital hip dysplasia. Stability consists of both bony and soft tissue components. The capsular model can be altered to simulate the redundant, thickened capsule seen in congenitally dislocated hips, and can also simulate the mechanical behavior of the capsule once the reduction has been obtained.

The "human" position commonly used for immobilization of the reduced hip affords both bony stability and capsular stability by eliminating redundancy in the capsule during twisting. The model demonstrates the effects of sectioning of the medial capsule to obtain open reduction by the Ferguson method, and the change in resultant force across the hip explains the persistant late dysplasia that is often seen clinically after such an approach. The role of the capsule in both innominate osteotomy (Salter) and femoral derotation osteotomies is clarified; these procedures alter both bony and soft tissue stability (Salter) or soft tissue stability alone (varus osteotomy) in a way which can be predicted by the model. Clinical implications are discussed.

Seventh Annual Meeting American Society of Biomechanics, Rochester, MN,
28 - 30 September 1983

AN ANALYTICAL STEREOPHOTOGRAMMETRIC METHOD TO MEASURE THE 3-D GEOMETRY OF ARTICULAR SURFACES

R. Huiskes and A. de Lange

Biomechanics Section, Lab. Exp. Orthopaedics, Univ. of Nijmegen
6500 HB The Netherlands

Accurate descriptions of the 3-D geometry of articular surfaces in skeletal joints have become essential information in several kinds of biomechanical investigations; e.g. (knee) joint model analyses, anthropometric studies, joint-contact region analysis, and cartilage biomechanics. The (optical or mechanical) methods previously applied to obtain these data are either expensive, tedious, or inaccurate. The measuring technique proposed here, based on analytical stereophotogrammetry, is believed to be a good cost-efficient compromise between accuracy and simplicity.

The method was tested on a known curved surface, and the influences of several error sources on inaccuracies in the end-results were evaluated, including choice of equipment, surface curvature, object positioning, and choice of co-ordinate reference system. It was found that a total inaccuracy (95% confidence interval) of 0.1 mm in the 3-D position of a surface point is feasible, a result which may be even improved at higher costs. However, under unfavorably chosen conditions (notably the use of an inaccurate 2-D co-ordinate digitizer to evaluate the stereo images), the total inaccuracy may go up to 1.5 mm.

This method was used to assess the geometry of knee-joint articular surfaces in vitro, the results of which will be presented and discussed. To represent the measured surfaces, 3-D computer graphics are applied. For this case, the precision of the method was estimated by repeated measurements.

It will be shown that this technique can also be used to measure the location-dependent thickness of articular cartilage, of course again in vitro, an illustrative example of which will be presented.

Computer Modelling of Proximal Femur Osteotomies

D.R. Pedersen and R.A. Brand
Orthopaedic Biomechanics Laboratory
University of Iowa Hospitals and Clinics
Iowa City, Iowa

Over the past few years we have developed techniques to study musculo-skeletal operations which alter the relationships of muscles, bones and joints [1-5] . Predictions of the mechanical effects of these operations on the joint loads and muscle force distribution are made, but the method does not account for any biological effects.

Kinematic data are generated by three triads of light emitting diodes, LEDs on the subject's hip, thigh and shank. By flashing the LEDs at a known frequency a time exposure will produce a time displacement history for each array. A mini-computer is used to control the cameras, flash the LEDs, and simultaneously record force plate, EMG and footswitch data. Biplanar radiographs of the subject's pelvis are used to determine the position of the pelvic array relative to pelvic bony landmarks. The LED, radiograph and anthropometric measurements are combined with the kinetic foot-floor reaction forces to calculate intersegmental resultant forces and moments. Anthropometric scaling techniques and non-linear optimization are used to distribute these intersegmental resultants to the muscles, ligaments and joints.

In this study the effects of several intertrochanteric femoral osteotomies are investigated. Ten, twenty, and thirty degree varus-valgus displacements, and ante-retroversion rotations of the proximal femur are effected. Assuming the desired result of surgical intervention is to help the patient achieve a normal gait pattern, these anatomic changes are introduced into the mathematical model with normal kinematic and kinetic data.

Comparing joint and muscle forces before and after the simulated surgeries showed little effect on the peak hip, knee and patello-femoral resultants. While three-dimensional hip force components remained within 5% of the presurgery predictions for all other situations, the anterior force on the femoral head ranged from 59% of normal in the 30 degree retroversion to 170% of normal in the 30 degree anteversion simulation. Anteversion of 30 degrees caused 19% and 10% increases in the gluteus minimus and medius and a 22% decrease from normal in the gluteus maximus. Thirty degree retroversion elicited 21%, 20% and 60% increases in these same three muscles. The rectus femoris and tensor fascia latae experienced a 33% increase after 30 degrees anteversion and a 33% decrease after femoral retroversion. These five muscles remained within 10% of predicted normal forces after varus-valgus displacement, except the gluteus minimus which reached 150% of physiologic force magnitude in the 30 degree valgus displacement model.

1. Crowninshield, R.D. ; Johnston, R.C. ; Andrews, J.G. ; Brand, R.A. : A Biomechanical Investigation of the Human Hip. Journal of Biomechanics 1978 Vol.11 p75
2. Crowninshield,R.D.; Brand,R.A.: A Physiologically Based Criterion of Muscle Force Prediction in Locomotion. Journal of Biomechanics 1981 Vol.14, No.11
3. Johnston, R.C.; Brand, R.A.; Crowninshield, R.D.: Reconstruction of the Hip. Journal of Bone and Joint Surgery 1979 61-A, No.5 p639
4. van Krieken, F.M.; Pedersen, D.R.; Brand, R.A.; Crowninshield, R.D.: Hip and Knee Muscle and Joint Force Predictions in Simulated Tumor Resections. Transactions of the Orthopaedic Research Society 1983 Vol.8 p300
5. Brand, R.A.; Crowninshield, R.D.; Wittstock, C.; Pedersen, D.R.; Clark, C,R. A Model of Lower Extremity Muscular Anatomy. Journal of Biomechanical Engineering 1982 Vol.104 p304

This work was supported in part by NIH grant AM14486.

PHOTOGRAMMETRIC MEASUREMENT OF INTERVERTEBRAL DISC DEFORMATION.

Ian A.F. Stokes and David M. Greenapple. University of Vermont, Department of Orthopaedics & Rehabilitation. Burlington, VT 05405 USA.

In this study we have investigated possible injury mechanisms to the surface fibers of the lumbar intervertebral disc. During compression of the disc, the endplates and attachment points of a fiber approximate. However, bulging of the disc may result in a longer path for each fiber. It has been assumed that this results in fiber stretch, and measurements of pressure distribution in the disc and mechanical model analyses support this. Torsion of the disc probably produces alternate positive and negative strain in adjacent layers of fibers. In this study we have made direct measurements in vitro of the amount of fiber strain.

Two calf lumbar discs and three human lumbar discs have been studied. Close range stereophotogrammetric non-contacting methods were used to measure the shape of a fiber on the surface of the postero-lateral part of the disc. A high degree of accuracy has been developed in the method of surface measurement. The path of the fiber was marked with microtargets 0.5 mm in diameter with a cross at the center. These were adhered to the annulus using cyanoacrylate cement. The spine segment was imbedded in dental plaster and loaded in a compression machine. Provision was made for compression and torsion loading of the specimen. Two cameras recorded the three-dimensional position of the marked points (the microtargets) on the fiber. The resulting films were enlarged and digitized for computerized analysis of the geometry of the disc. In three tests of the accuracy of measurement, a standard error of 0.1 mm was found, equivalent to 0.75% strain over a fiber length of about 15mm.

In each test, four parameters were measured: the compressive load, the axial compressive deformation, the radial bulge of the disc and the length of the marked fiber. Discs were studied while being compressed at a rate of 2 mm per minute, under compressive loads up to 2.5kN or static torques up to 17Nm.

Results were in a form which could be compared with the mathematical model predictions of Broberg and von Essen (Spine 5:155-167, 1980). This model predicts the behavior of a 'constant volume disc' which is one in which there is no fluid loss from the disc or deformation of the endplates.

Very little stretching of the surface annular fibers was measured in six of seven compression tests. In only one test a +3% strain was recorded at 2.5kN. In all other tests the strain was less than 2%. The radial bulge was less than predicted by the 'constant volume' model. Together, these findings suggest that fluid loss and endplate deformation prevent annular fiber strain in slow pure compression of the disc. In the tests with torsional loads, a torque of 17 Nm. produced a strain of positive or negative 4%, depending upon the direction of the torque in all three tests on two discs.

We have concluded that under pure compression alone, and despite the bulging of the disc surface, that there is very little strain of the disc surface. Significant strains are produced under torsional loading, and may also occur in more rapid compression loading, and in complex bending configurations.

COMPRESSION STUDIES IN THE HUMAN THORACOLUMBAR SPINE

By A. Sances, Jr., D.J. Maiman, J.B. Myklebust, S.J. Larson, J.F. Cusick, M. Chilbert, R. Jodat, C. Ewing, and D.J. Thomas

Medical College of Wisconsin, Marquette University, and Veterans Administration Center, Milwaukee, WI

INTRODUCTION

Injuries sustained by compression in functional or single units have been reviewed by others.[1,2,3] The force magnitudes and energy levels for compression injuries have been well described for these units, however, little information is available for the total thoracolumbar column.[4,5] For further study of these mechanisms, 14 male isolated ligamentous thoracolumbar spines and 4 intact male human cadavers were studied.

METHOD AND RESULTS

All specimens were determined to be within normal limits by medical history and x-ray examination conducted prior to the tests. Tissues were x-rayed and spinal injury was determined by careful gross dissection and confirmation by clinical staff members. Supporting tissues were carefully removed to avoid damage to the ligaments. All studies were done in preparations where the tissues were kept at 2° C until studied within 1-3 days following death. The 14 male isolated ligamentous thoracolumbar spines were mounted at the upper and lower segments at T2-T3 and L5-sacrum in methyl methacrylate and molded into 15 cm diameter aluminum cylinders with fixation rods driven into the tissues. All specimens were preflexed, and vertical forces were applied with an MTS electrohydraulic servo system at rates of 1-12 cm per second. The intact cadavers were seated, preflexed, fixed at the pelvis, and vertical forces were applied at the T1-T2 region with a 15 x 15 cm flat plate. A free body diagram of the relevant forces and distances was developed for the externally applied force to the intact cadaver.

The isolated thoracolumbar columns failed in the lower thoracic and upper lumbar regions at forces of 1100 to 5000 Newtons. Forces ranging from 800 to 2000 Newtons produced compression fractures of the midthoracic vertebral bodies of the isolated thoracolumbar sections. In two spines the cervical elements were included. In these preparations, failures occurred in the upper thoracic spine at 556 and 800 Newtons. The angle between the fractured elements was 30-40°.

The intact cadaver spines failed in the low thoracic and upper lumbar regions at forces between 1100 and 2800 Newtons. Failure angles ranged between 28 and 50°.

The length of the column correlated with failure load and distance from the point of rotation to the line of applied force. A free body model of the intact cadaver study indicates that for 445 Newtons applied to the upper thoracic region, force in the posterior ligament complex is approximately 2000 Newtons and that the lower vertebral body is approximately 2900 Newtons.

REFERENCES

1. Liu YK: Biomechanics and biophysics of CNS trauma, in Central Nervous System Trauma Research Status Report, G.L. Odom (ed), Duke University, Durham, NC, 1979, p. 36.
2. Kazarian L, Graves GA: Compressive strength characteristics of the human vertebral centrum, Spine 2(1):1-14, 1977.
3. Lin HS, Liu YK, Adams KH: Mechanical response of the lumbar intervertebral joint under physiological (complex) loading, J Bone Joint Surg 60A:41-55, 1978.
4. Sances A Jr, Myklebust JB, Maiman DJ, et al: The biomechanics of spinal injuinjuries, CRC Crit Rev Bioeng, In Press.
5. Sances A Jr, Myklebust J, Houterman C, et al: Head and spine injuries, AGARD Conf Proc No. 322 on Impact Injury Caused by Linear Acceleration: Mechanism, Prevention and Cost, Koln, Germany, April 26-29, 1982, pp. 16-1 - 16-11.

Supported in part by ONR Contract No. N00014-77-C-0749

The Effect of Gender on the Strength Characteristics of Squirrel Monkey Vertebral Bodies

S. D. Smith-Lagnese
Leon E. Kazarian

Air Force Aerospace Medical Research Laboratory
Aerospace Medical Division, Air Force Systems Command
Biodynamic Effects Branch
Wright-Patterson Air Force Base, Ohio 45433

ABSTRACT

The present effort was initiated to determine correlations between rate, position, geometry, and strength characteristics of isolated female Squirrel monkey vertebral bodies. The results were compared to a previous investigation accomplished on male Squirrel monkey vertebral bodies to determine the effect of gender on various mechanical and structural parameters. All Squirrel monkeys used in this experiment were approximately the same age.

The spinal columns of eight young adult female Squirrel monkeys were dissected en masse. The vertebral bodies were separated at the intervertebral joint. All transverse and posterior elements were removed and the remaining vertebral centra cleaned of all soft tissue. Fifteen vertebral bodies from each spine were obtained in this manner. To insure consistent uniaxial compressive load application, select material was trimmed from the inferior and superior surfaces of the specimens using a Buehler Isomet Low Speed Bone Saw. This trimming technique was developed and tested on the male specimens and found to greatly aid in generating consistent load configuration and strength results. The specimens were loaded in compression according to a test matrix at displacement rates of 0.1, 1.0, and 2.0 in./min.

As found in the results on the male Squirrel monkey, column position had the most obvious effect on both the geometry and strength parameters. Both the average surface area and average height increased with position and indicated a linear relationship. Although the area and height data appeared consistently lower in the female than in the male, the slenderness ratios were relatively higher in the female and showed the sharp increases between column positions P_3 and P_5 found in the male results.

The strength parameters including the average stiffness and average ultimate load increased with column position. The calculated stress and strain behaved accordingly. All strength parameters observed for the female excepting the displacement and strain results were slightly lower than those results observed in the male; however, the females did show the observed similarity in column effects between the strength parameters and the slenderness ratio.

The rate effect was less pronounced but slight increases in ultimate and yield loads were observed. Average stiffness did not vary with rate.

It appears that strength differences in the vertebral bodies between male and female Squirrel monkeys are subtle and appear as slight differences in magnitude and not necessarily in their rate or position dependent behavior. The similarity between the position dependent tendencies of the slenderness ratio and the strength parameters suggests a role between kinetic and kinematic behavior and spine stabilization.

MEASUREMENT OF INTRACOMPARTMENTAL PRESSURE IN THE BACK

D. Carr, M.D., J.W. Frymoyer, M.D., L. Gilbertson, B.S.,
M.H. Krag, M.D., and M.H. Pope, Ph.D.
Department of Orthopaedics and Rehabilitation
University of Vermont College of Medicine

We propose that the erector spinae muscles can develop a "compartment syndrome" within their enclosing lumbodorsal fascia. No previous description of such a compartment could be found. We measured for the first time intracompartmental pressure (ICP) in normal volunteers and investigated the pertinent anatomy.

METHODS: Eight volunteers had slit catheter ICP measurements done five cm lateral to the L3 spinous process. Loads used were (1) antigravity with and without a Valsalva maneuver for postures of 20° extension, upright standing, 30° flexed and 90° flexed; and 2) 80% of maximum voluntary extension effort (MVEE) for 30° of flexion. The latter load was performed isometrically against a strain-gauged cable attached to a chest harness with the pelvis stabilized. This load was initially applied for two minutes followed by a 3 minute rest and then a second 1 minute effort. Reproducibility studies were done. RESULTS: A mean opening upright ICP of 4.9 mm Hg was obtained with no pressure change for any position except 20° extension ($p < 0.01$). Valsalva increased the ICP in all positions except 90° flexion ($p < 0.02$). MVEE produced a significant increase ($p < 0.01$) compared to upright and 30° flexed. ICP during sustained 80% MVEE steadily increases during the initial 2 minute effort and returns to baseline promptly (< 3 seconds) with relaxation. The second MVEE attained the same initial ICP but the trend was for an increased slope. Anatomic dissection confirmed human cross sectional studies and CT scans in defining a well enclosed lumbodorsal compartment. CONCLUSIONS: 1. We found that significant intracompartmental pressures (ICP) exist in the region occupied by the erector spinae muscles. 2) ICP changes with posture, Valsalva maneuver, trunk extension effort, time; and these changes are reproducible. 3. ICP changes were similar to those seen in other body regions in which exertional compartment syndromes are known to occur. 4. Our anatomic studies indicate that the erector spinae muscles exist within a closed anatomic space. 5. We hypothesize the existence of a "lumbodorsal compartment syndrome" as a possible new subtype of low back pain. 6. ICP of the lumbodorsal fascia compartment may play a significant role in the biomechanical functioning of the human spine. Its relation to intra-abdominal pressure and trunk muscle activity is under investigation.

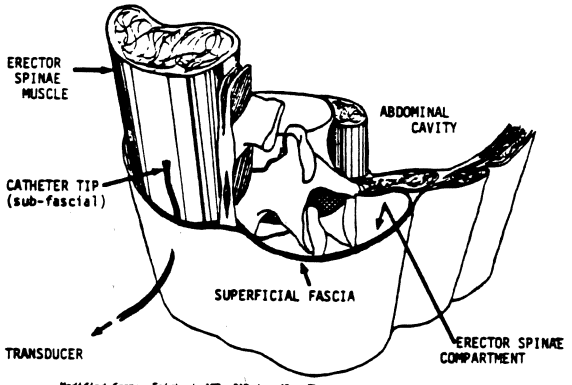

Modified from: Fairbank JCT, O'Brien JP: The abdominal cavity and thoraco-lumbar fascia as stabilisers of the lumbar spine in patients with low back pain. I Mech E Conf Proc p 76, 1980

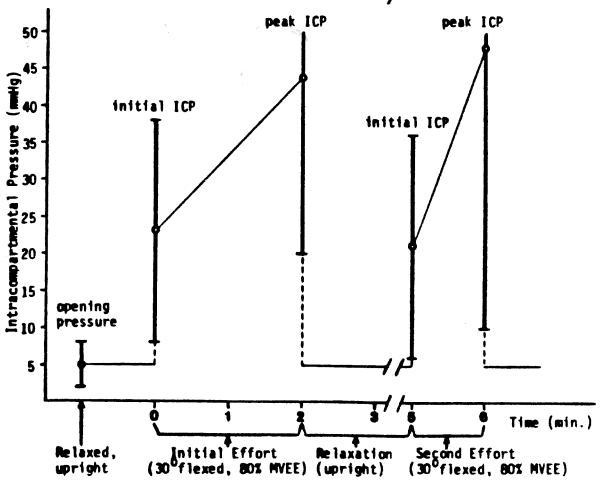

EFFECT OF IMMOBILIZATION AND REMOBILIZATION ON THE PROPERTIES OF THE MEDIAL COLLATERAL LIGAMENTS

Savio L-Y. Woo, Ph.D., Peter O. Newton, B.A., Mark A. Gomez, M.S.

San Diego Veterans Administration Medical Center
and
University of California, San Diego
La Jolla, California 92093

The effects of immobilization and remobilization on the knee joint and its periarticular connective tissues are of significant clinical interest. The subject has been studied by several investigators, but the data on the changes of mechanical properties of the ligament substance are lacking.

In this study 22 New Zealand white rabbits each weighing approximately 30 Newtons were used. For immobilization, a 2.4 mm diameter Steinmann pin was used to force the left knee into flexion (1). For remobilization the fixation pin was surgically removed. Four groups were evaluated: 1) 9 wks of immobil., 2) 12 wks of immobil., 3) 9 wks immobil. + 9 wks. remobil. and 4) 12 wks immobil. + 9 wks remobil. At sacrifice, the medial collateral ligament (MCL) specimen including the bones, were excised. The clamping and tensile testing procedure have been described in Woo, et al (2). The load-deformation curve for the MCL-bone complex and the load-strain curve of the MCL substance were obtained.

With immobilization the strength characteristics of the MCL-bone complex of knees from Group 1 animals reduced to approximately 1/3 that of the contralateral non-immobilized controls. Further reduction in strength from Group 2 animals was found. There were large differences in the load-strain curves between the control and experimental MCL's indicating that changes in the ligament mechanical properties had possibly occurred. Previous work by our laboratory indicated that the MCL from Group 1 had no significant changes in collagen mass, i.e. increase in collagen degradation in the immobilized MCL (14 ± 6% over control) was balanced by the increase in new collagen formation (11 ± 3%). However, the Group 2 MCL's had significant ligament atrophy (3).

Interestingly, the load-strain curves of the exp. and control MCL from Groups 3 and 4 were similar indicating that the recovery of the properties of the MCL substance was quite rapid. The structural strength of the MCL-bone complexes from the exp. knees, however, continued to be inferior.

It appears that there is a general relationship between stress and motion deprivation on tissue remodeling, i.e. alteration in its mechanical properties as well as atrophy. The structural caliber of the ligament-bone junction also becomes significantly inferior. It can be safely said that the duration of stress deprivation must also play a significant role. In terms of recovery, the properties of the MCL substance in the functional range appear to recover rapidly, whereas the properties of the MCL-bone complex continue to be lower than that of the normal (4).

1. Akeson, et al: Clin. Orthop. 93:356, 1973.
2. Woo, et al: Arth. and Rheum., 18:257-264, 1975.
3. Amiel, et al: Clin. Orthop., 172:265-270, 1983.
4. Noyes, et al: J. Bone Joint Surg., 56A:1406-1418, 1974.

This work is sponsored by Rehabilitation R&D of Veterans Administration and NIH Grant AM14918.

THE IMPORTANCE OF VASCULARITY AND CONTINUOUS MOTION IN BIOLOGICAL LIGAMENT SUBSTITUTION

D.L. Butler, F.R. Noyes, E.S. Grood, M. Siegel,
M.L. Olmstead*, R.B. Hohn* and R. Kaderly*
Dept. of Orthopaedic Surgery, University of Cincinnati, Cincinnati, Ohio 45267
and *Dept. of Veterinary Clinical Sciences,
Ohio State University, Columbus, Ohio 43210

INTRODUCTION Anterior cruciate ligament (ACL) substitution continues to be a common problem for orthopaedic knee surgeons. A review of the literature over the past 60-70 years points to both the number of different soft tissues used (tendon, fascia, menisci) and the mixed clinical results obtained (1). Recently certain factors have been identified as critical to the success of such replacement procedures (2). Among them is the need to return the graft tissue to normal vascularity as rapidly as possible (2,3). More recently, continuous passive motion (CPM) has also been advanced as an important modality (4). In this study, each is examined in the primate.

METHODS Seventy-five male cynomolgus monkeys weighing 4.8 $\pm$ 0.1 kg ($\bar{X} \pm$ SEM) were employed. Group I (n=9) were controls. Group II animals (n=40) were used to examine the effects of vascularity and postoperative casting on graft properties and in Group III (n=26), vascularity in the presence of continuous motion. In the casted group, grafts were evaluated at 6,13,26 and 52 weeks post-op and compared to controls. In the other group, continuous motion was performed for three weeks after surgery before evaluation at 13 and 26 weeks. In both groups, a free autogenous patellar tendon-bone unit (free graft or FG) was used to replace the anterior cruciate on one side and a vascularized patellar tendon-bone unit (VPT) on the other. Histologic and vascular changes were evaluated separately. Surgical procedures were alternated to eliminate left-right differences.

In the mechanical test groups, hindlimbs were removed after sacrifice and quantitative laxity measurements performed. Graft and ligament dimensions were then taken. Specimens were mounted, marked with ink for surface strain measurement and failed at a strain rate of 100%/s.

RESULTS Total anterior-posterior laxity in the knees was found to be 160% of control by 6 weeks in the cast group but returned to control values by one year. Joint range of motion and cartilage integrity were better in those knees receiving CPM than those casted post-op. Cast group stiffness and maximum load for the FG and VPT showed monotonic increases from 15% of control ACL at six weeks to 37-43% by one year. No significant differences were noted between FG and VPT at any of the time periods. Also no significant differences could be seen in graft performance between the cast and CPM groups at 13 weeks.

DISCUSSION ACL replacement is obviously affected by many biological and surgically-related factors. Our results suggest that, in this animal model, vascularity provides no significant advantage to graft performance at the time periods evaluated. Similarly three weeks of continuous passive motion produced no distinct improvement in the mechanical properties of the graft at thirteen weeks post-op, although its benefit to the joint was noteworthy.

REFERENCES 1) Butler, D.L. et al, 25th ORS, p. 81, 1979; 2) Noyes, F.R. et al, Clin. Orthop., 172, pp. 71-77, 1983; 3) Noyes, F.R. et al, J. Bone Jt. Surg. (in press); 4) Salter, R.B. and Minster, R.R., 28th ORS, p. 225, 1982.

This work was supported in part by NIH grants AM27517 and AM00965.

THE FUNCTIONAL RELATIONSHIP BETWEEN STRAIN IN THE POSTERIOR OBLIQUE FIBERS AND THE PARALLEL, LONG FIBERS OF THE HUMAN KNEE MEDIAL COLLATERAL LIGAMENT

Richard A. Fischer, MD, Steven W. Arms, BS, Malcolm H. Pope, Ph.D., Robert J. Johnson, MD., University of Vermont, Department of Orthopaedics & Rehabilitation, Burlington, VT 05405

Introduction: The anatomy of the triangular flare of collagen fibers immediately posterior to the long, parallel fibers of the human knee medial collateral ligament (MCL) is controversial. This structure, the "posterior oblique ligament" (POL), is said by some to be separate from the MCL with different bony attachment points, whereas others regard the POL as being part of the MCL. This study was an attempt to resolve this controversy.

Materials and Methods: Using a Hall strain transducer effect device we investigated the effect of the POL on strain in the long parallel fibers of the MCL as a function of knee flexion angle. The device was sutured to the long parallel fibers of the MCL and change in the Hall effect voltage output, as the MCL elongated and shortened, was recorded on an x-y plotter. We included 10 knees from human cadavers in this study. The mean age was 59.6 years. The ipsilateral femur of each subject was rigidly fixed to a table via skeltel fixation and Hoffman clamps. The MCL was exposed through a mid-medial incision and the strain device was attached at various locations on the superficial MCL. Each knee was passively flexed from 0° to 120°, first with no applied torque, then with a valgus moment of 44.5 N at the medial malleous and finally with an external rotation torque of 13.6 Nm applied to an axial coupling fixed to the distal tibia. Then a series of three incisions were made parallel to the posterior margin of the long fibers of the MCL, and after each cut the knee was similarly tested. The first incision was made superior to the medial joint line. The other two incisions were extensions of the first incision, resulting in the complete separation of the POL from the long parallel MCL fibers.

RESULTS: The effect of the surgical incisions on strain in the long fibers of the superficial MCL was variable depending on the position of the transducer on the ligament. With the transducer placed anteriorly on the MCL at the joint line the more the POL fibers were separated from the long parallel fibers of the MCL, the greater the increase in strain to valgus and external rotation, with net increases in strain above the normal baseline of .78% in valgus and .61% in external rotation. This increase in strain was markedly less when the transducer was placed posteriorly on the MCL at the joint line. When the transducer was attached superiorly to the joint line, net decreases in MCL strain of up to 1.85% in external rotation were noted after sectioning away the POL. In one knee it was later discovered that no anterior cruciate ligament (ACL) was present and a marked increase in strain its superficial MCL was demonstrated with subsequent separation from the POL. The net increase in this strain from the original baseline was 3.65% in external rotation and 5.25% under Valgus stress. Maximum strain in this knee prior to sectioning was 4.70% above the baseline with valgus moment. After separation from the POL, the maximum strain above baseline was 9.95% under valgus stress.

Discussion: The results of this study demonstrate that the posterior oblique fibers of the superficial MCL affect the strain pattern of the long fibers of the superficial MCL. When these posterior fibers are surgically separated from the long parallel fibers, strain in the MCL was demonstrated to either increase, or decrease depending on which position of the MCL is used as a reference. Anatomically, the posterior oblique fibers of the MCL pull the long parallel fibers of the MCL posteriorly and inferiorly, at positions superior to the joint line. Inferior to the joint line, the oblique fibers would tend to pull on the parallel MCL fibers in a posterior/superior fashion. Relaxation of this posteriorly-directed stress via the surgical incisions, could explain why strain decreases in the superior positions of the MCL in this study, even though valgus force and external rotation torque are applied to the knee. It appears that functionally the posterior oblique fibers of the superficial MCL are intimately related to the long parallel fibers of the MCL.

ACKNOWLEDGEMENT: This study was supported by NIH grant #PHS RO1 29665-01.

SURFACE STRAINS IN HUMAN PATELLAR TENDON-BONE UNITS

D.C. Stouffer, D.L. Butler*, and R.F. Zernicket
Dept. of Aerospace Engineering & Applied Mechanics and *Giannestras Biomechanics Laboratory, University of Cincinnati
†Department of Kinesiology, University of California, Los Angeles

SUMMARY Axial failure tests were performed on patellar tendon-bone units. High speed film analysis revealed larger surface strains near the bone insertions than in the midsection. A constitutive equation is advanced to explain these variations; one based on the varying crimp pattern along the tissue length. The model is used to predict both average and local strains during deformation.

INTRODUCTION Large differences have been noted in reported strains for both ligament and tendon-bone units. When based on bone-to-bone displacement, strains at maximum stress have typically exceeded 20 to 40% [1,2] while local mid-substance strains using optical and Hall effect devices have yielded only about 5-7% [3,4]. The differences have to date not been explained. A model is proposed, based on physical measurements and mechanical tests, which might help explain some of the discrepancies.

METHODS Eight tissues were examined. Four patellar tendon-bone units from three human donors (X=28) were marked with tranverse ink bands, mounted in specially designed grips and failed in tension at a strain rate of 100%/s. Variations in local strains from digitization of high speed films were plotted as peaks proportional to local strains. Values near the proximal and distal insertions were an average 2.5 times the local strains in the midregion. Detailed histology performed on a fifth specimen revealed a fiber bundle crimp frequency near the insertion site 1.5 + 0.2 ($\bar{X}$ + SEM) times that in the midregion. The shape of the crimp near the insertion was also found to be more "pinched" at the corners than the sawtooth appearance seen in the tissue midregion.

CONSTITUTIVE MODEL While several crimp shapes have been proposed, our model is a modification of those suggested by Kastelic et al [5] and Diamant et al [6]. The model consists of a multi-element configuration such that between corners there are three links connected by two flexible nodes, each with rigidity, k_2. Corner rigidities are set equal to k_1. By relating node rigidity to bending moments and isolating the angles, ϕ_1 and ϕ_2, between the links in the deformed state, the strain parallel to the fiber bundle can be expressed as

$$\varepsilon_x = (1-\alpha)[1 + F/AE \cos\phi_2] \cos\phi_2/\cos\theta_0 + [1 + F/AE \cos\phi_1] \cos\phi_2/\cos\theta_0 - 1$$

where F, A, E and θ_0 are force, area, modulus, and initial crimp angle, respectively.

RESULTS AND DISCUSSION The model reveals maximum strains of 60-65% at the fiber bundle insertion sites into bone and midsubstance values are only about 3-9%. These predictions are also consistent with the unfolding sequence observed under the microscope during low load testing on additional fascicle specimens.

REFERENCES 1. Noyes, F.R. and Grood, E.S., J. Bone Jt. Surg., Vol. 58-A, 1976, pp. 1074-1082. 2) Butler, D.L. and Stouffer, D.C., J. Biomech. Eng., May, 1983. 3) Arms, S. et al., 28th ORS, 1982. 4) Woo, S.L-Y, Biorheology, Vol 19, 1982, pp. 385-396. 5) Kastelic, J. et al., J. Biomech., Vol 13, 1983, pp. 887-894. 6) Diamant, J. et al., PRS Lond. B. Vol. 180, 1972, pp. 293-315.

This work was partially supported by NSF grant MEA-8118140 and by NIH grant AM00965.

A Computerized Three-Dimensional Biomechanical Static Strength Prediction Model for Studying Stresses from Manual Materials Handling Operations

Arun Garg
Industrial and Systems Engineering
The University of Wisconsin--Milwaukee
Milwaukee, Wisconsin 53201

Don B. Chaffin
Industrial and Operations Engineering
The University of Michigan
Ann Arbor, Michigan 48109

It is the intent of this paper to describe and demonstrate a method developed at The University of Michigan to evaluate the biomechanical stresses induced by common manual materials handling activities in industry. The biomechanical strength model considers the body to be a system of rigid links having a fixed length, mass and center of gravity. A biomechanical analysis of a manual materials handling task requires:

(i) simulation of the body posture used to perform the task,

(ii) computation of forces and moments at various body joints due to forces acting at the hands and the body segment weights, and

(iii) comparison of the forces and moments with volitional forces and moments (muscle strength) to estimate the fraction of the male and female populations that could be expected to perform the task without exceeding muscle strength.

The input to the model requires specifying a gross body posture (such as stoop, squat, stand, lean, etc.), magnitude of hand forces, task (such as lift, push, pull, etc.) and either the coordinates of the hands with respect to the ankles or the body joint angles. The output from the model includes a graphical representation of the body posture, fractions of the male and female populations that can be expected to perform the job without exceeding muscle strength, three different limiting muscle strength groups, an estimate of compressive force at the L5/S1 disc, and the action limit and the maximum permissible limit recommended by NIOSH. The model can be used either in an interactive mode or a batch processing mode.

The use of such a methodology identifies specific physical acts required in a job which are highly stressful. Thus, alternative job methods can be evaluated or restrictions may be placed on the employment of weaker individuals. In many cases, injury and illness records confirm the type of injury potential predicted by the biomechanical model.

Clearly the biomechanical model is a simplistic representation of the complex mechanics of the body. Applications and limitations of the model, along with some case studies, are discussed. Differences between isometric strength and dynamic strength based on a psychophysical methodology are also discussed.

MODELING AN ACTIVE NEUROMUSCULATURE RESPONSE TO MECHANICAL STRESS

Andris Freivalds, Department of Industrial & Management Systems Engineering, The Pennsylvania State University, University Park, PA 16802
Ints Kaleps, Modeling & Analysis Branch, Biodynamics and Bioengineering Division, Air Force Aerospace Medical Research Laboratory, Wright-Patterson AFB, OH 45433

INTRODUCTION - The use of biodynamic computer-based models for the prediction of human body response to mechanical stress such as high-G acceleration or crash impact, has become an extremely useful and cost-effective research and developmental tool, especially as an alternative to direct experimentation with humans and animals. One such model, the Articulated Total Body (ATB) Model, uses rigid-body dynamics with Euler equations of motion and Lagrange type constraints to simulate human body reponses. Originally developed by Calspan Corp. for the study of human-body and anthropomorphic dummy dynamics during automobile crashes for the U.S. Department of Transportation [1], the ATB Model has been since adapted for use by the Air Force to simulate whole-body articulated motion resulting from abrupt accelerations or impacts [2].

The ATB Model, although realistically reflecting human body structure, mass distribution and tissue material properties, presently has the serious limitation of only simulating events with passive internal responses. To faithfully represent human data including both voluntary and reflex responses to external force, one must include the modeling of an active neuromusculature.

METHODOLOGY - The study utilized a model configuration with 15 body segments and the 14 joints between the segments. To incorporate muscle elements into the model, the harness/belt routine [3] was utilized. Instead of attaching the harness end points to external structures, they were incorporated within the body. The existing functional form of the harness routine consisted of four polynomial terms in strain (ε) and strain rate ($\dot{\varepsilon}$):

$$F(\varepsilon,\dot{\varepsilon}) = F_1(\varepsilon) + F_2(\varepsilon)F_3(\dot{\varepsilon}) + F_4(\dot{\varepsilon})$$

and allowed the use of a lumped three-parameter muscle model. F_1 corresponds to the parallel elastic element consisting of the sarcolemna and connective tissue and accounts for passive stress-strain effects. F_2 and F_3 correspond to the contractile element consisting of the actin-myosin cross-bridges and accounts for the length-tension and force-velocity relationships. F_4 corresponds to the damping element consisting of fluid-filled fibers and accounts for passive viscous damping forces.

RESULTS - Three validation studies were performed. The first simulated elbow flexion with one muscle/harness system representing the elbow flexors. The results indicated that the force-velocity effects produced the greatest changes in muscle force, with significant force changes due to the damping element and length-tension relationship and no force changes due to the parallel-elastic element. The second study simulated elbow flexion using three muscles: biceps brachii, brachialis and brachioradialis. Alteration of origin and insertion distances by 10% of the distance changed the muscle forces only slightly. The third study simulated the whole body response to a 2-G_y lateral force utilizing trunk musculature. Although the musculature did not completely prevent the lateral deflection of the body, the response was significantly delayed compared to a control response.

[1] Fleck, J.T., F.E. Butler and S.L. Vogel, An Improved Three Dimensional Computer Simulation of Motor Vehicle Crash Victims, TR No.ZQ-5180-L-1, Calspan Corp. 1974.
[2] Fleck, J.T. and F.E.Butler, Development of an Improved Computer Model of the Human Body and Extremity Dynamics, AMRL-TR-75-14, 1975.
[3] Butler, F.E. and J.T.Fleck, Advanced Restraint Systems Modeling,AMRL-TR-80-14,198

SPECTRAL ANALYSIS OF PARASPINAL EMG FATIGUE CHARCTERISTICS

Malcolm H. Pope, PhD, Dwight Keller, MD
Dennis Donnermeyer, BMET, David Wilder, MSME
Department of Orthopaedics & Rehabilitation
University of Vermont, Burlington, VT 05405 USA

Introduction: The spinal musculature is the major support of the spine. Fatigue of those muscles could lead to an increased susceptibility to injury. The electromyogram (EMG) is used to measure muscle activity. It is a complex signal arising from the summation of asynchronously firing motor units, which can be recorded through surface electrodes. It was not until about 15 years ago that the interpretation of the signals using power spectrum analysis was used as a method of quantitative measurement of fatigue (1-5).

Methods: We conducted static fatigue exercise tests of the erector spinae muscles. The center frequency of the Fourier Power Spectrum of the EMG signal was used as a method to assess muscle fatique. Five male subjects with no history of back problems were used in these experiments. The tests were conducted in a seat belt restrained sitting position with a femur to back angle of 70-80°. A chest harness was worn which tranmitted the horizontal forces from the torso to a vertical support. The force exerted was monitored by a load cell and was displayed on a digital read-out. All subjects were informed of the experimental procedure and given one day of training to become acclimated to the test. Five days of fatiguing tests with constant load held until exhaustion were conducted at 80,60,45,37.5 30% of the subjects Maximum Voluntary Contraction (MVC). Prior to each day's fatiguing test, 3 MVC efforts were performed using the maximum as the 100% index. Also prior to the fatigue tests, subjects held for a few seconds, various loads which were percentages of their MVC.

Results: EMG spectral activity was determined at the beginning and end of the five fatiguing tests. The center frequency of the power spectrum (of a 0-250 Hz frequency spectrum analysis window) was determined over a 6 second sample period. The mean center frequencies decreased significantly between the beginning and the end of the fatigue test for all tests except the 60%
and 45% MVC. From the right paraspinal muscles Root Mean Square EMG activity was compared to the load sustained. From the left paraspinal muscles, EMG activity and load sustained were each integrated over a period of one second. These data analyses were applied to all the static tests where the subjects held a percent of their MVC for only a few seconds. The population (all subjects tested) data showed a linear relationship between EMG activity and load. However, individually some subjects showed a linear relationship between EMG and load and others showed a logarithmic (or non- linear) relationship between these variables.

Conclusions: This study confirms that the center frequency shift of the EMG power spectrum associated with muscle fatigue during isometric efforts can be observed in the erector spinae muscles. The characteristic EMG changes have provided a non-invasive, quantitative and objective indicator for assessing muscle fatigue. Each subject has a unique EMG vs. load relationship which may differ from others or the population.

Acknowledgement: This work was supported by Grant No. USDAMD 1782C-2153 from Army Aeromedical Research Laboratory, Fort Rucker, Alabama.

Bibliography

1. Lindstrom LR, Magnusson R, Petersen I: Muscular fatigue and action potential conduction velocity changes studies with frequency analysis of EMG signals. Electromyography 10: 341-356, 1970.
2. Lindstrom L, Kodefors R, Peterson I: An electromyographic index for localized muscle fatigue. J. Appl. Physiol. 43:750-754, 1977
3. Petrofsky JS: Computer analysis of the surface EMG during isometric exercise. Comput. Biol. Med. 10:83-95, 1980
4. Petrofsky JS, Dahms T, Lind AR: Power spectrum analysis of the EMG during static exercise. The Physiologist 18:350, 1975
5. Viitasalo J, Komi P: Signal characteristics of EMG during fatigue. Eur. J. Appl. Physiol. 37:111-121, 1977

CONSTRUCTION OF A POLICE PHYSICAL FITNESS BATTERY AS A SUBSTITUTE FOR AGE REQUIREMENTS

Richard A. Mostardi, James Porterfield, Stanley Urycki

Three hundred and fifty-six members of the Akron City Police Department volunteered for this project, the purpose of which was to answer the question concerning maximum age and police officer cardiology. The officers were examined by a staff of professionals at Akron City Hospital utilizing a job oriented battery of tests. Concurrently a job analysis was done. It was theorized that the average energetics of the job would be similar to the average energetics as measured in the laboratory, in which case an age stratified series of tests could be used in place of maximum age.

However, the job analysis indicated that the average energy demands of police work are very low and could be met by most individuals. Conversely the medical testing showed that most of the officers were average with respect to musculoskeletal and cardiopulmonary energetics. This combination of facts precluded the establishment of a maximum age requirement at the entry level. Instead the large data base was reduced, through statistical processes of Factor Analysis, Kaiser Factor Matching and multifactor linear regression to a few variable that could be replicated in the laboratory and were repeatable.

These tests were the graded exercise test and the Cybex test for musculoskeletal strength. Fortuitously, these two tests accounted for 54% of the total variance of the data matrix. Factor scores were then calculated for the 10 factors and these were entered into a linear regression equation predicting age. The factor series and regression coefficients will serve as the basis for testing entry level officers. These statistical values have measures of variance, the lower limit of which will be used as the cut-off for acceptance of an individual into the police program. This method imploys job related tests, has coefficients generated from a substantial sample size, and is independent of age. This process appears to be a sound scientific approach for hiring, is equitable to employee and employer and is legally defendable.

QUANTITATIVE ANALYSIS OF FOREARM MUSCULATURE

R. M. Gross, E. Y. Chao, K. N. An
Orthopedic Biomechanics Laboratory Mayo Clinic

In 1973, R. H. Jensen developed a method to provide quantitative information of human thigh muscles. In 1974, G. T. Rab applied this method to study the forces across the lumbar spine.

The main objective of this study is to use a similar technique to develop a quantitative muscular model of the forearm. This model allows for the calculation of forces at different levels of the forearm and wrist. It will also provide essential insight to the functional anatomy of the forearm.

Cadaver forearm specimens were imbedded in wooden boxes, suspended and secured by self-curing resin. The boxes were then serially sectioned at 1.0 and 0.5 centimeter intervals. The cross-sectional view allowed the reconstruction of the forearm muscles in space. The cross-sectional area, centroid, and the volume for each muscle could be obtained. The data are expressed in terms of the adjusted physiological cross-sectional area, PCA (muscle volume divided by length). Forearms oriented in pronation, neutral and supination were studied and the results were obtained.

Despite the anthropometric variation among the specimens studied, remarkable consistency in the relative size of all the muscles was found. These data are expressed in dimensionless terms (see table below). The force of each muscle could be espressed as percent of total muscle volume or the percentage of the physiological cross-sectional area. From the model, a relative force analysis for each individual muscle was performed to determine the percentage of contribution to the functional capability of the wrist.

The muscle volume distribution is not significantly affected by the forearm position. However, relative orientation of certain muscles is significantly changed from full pronation to full supination position. This change may produce significant effects in the forearm bone loading under isometric contrations of extrinsic muscles. The present results were compared with that produced previously by Fick. Although no close agreement has been found, the general trend and distribution of these muscles in the forearm is quite similar. The disagreements in the magnitude could be attributed to the different techniques used in determining the cross-sectional area and the different technique used to determine the various moments.

From the results of this study, the following conclusions were made. 1) An accurate and quantitative forearm musculature model has been developed. 2) The model is flexible enough to adjust to advances in muscle physiology. 3) Important functional relationships can be described from this data. 4) In spite of the anthropometric variation of the specimens used, remarkable consistency in the relative size and centroid line orientation of all the muscles was found. 5) The muscle volume and PCA did not change significantly by the forearm position but the orientation of certain forearm muscles was altered. 6) The results produced in this study can provide valuable information to the treatment of forearm impairments. The muscle volume distribution is not significantly affected by the forearm position. However, relative orientation of certain muscles to the forearm bones are significantly changed from full supination to full pronation.

VOLUME & PCA DISTRIBUTION OF FOREARM MUSCLES (n=4)

	Vol%	PCA%		Vol%	PCA%
Flexor Carpi Radialis	7	8	Extensor Digitorum Communis	7.5	7.0
Flexor Digitorum Superficialis	17	15	Extensor Digitorum Minimi	2	2
Flexor Carpi Ulnaris	8.5	7	Extensor Carpi Ulnaris	5	5
Flexor Digitorum Profundus	22	18	Extensor Pollicis Longus	2	3
Flexor Pollicis Longus	5	6	Extensor Indicis Proprius	2	3
Palmaris Longus	2	3	Adductor Pollicis Longus	3	5
Extensor Carpi Radialis	15	15	Extensor Pollicis Brevis	2	3
			Total	100	100

Department of Orthopedic Surgery - Mayo Clinic

Mechanical Efficiency of Overarm Throw in Handball[1]

Hiroh Yamamoto[2] and Marlene Adrian (Washington State University, Dept. of Physical Education for Women, Pullman, Washington 99164-1512)

The purpose of this study was to investigate the mechanical efficiency of the overarm throw in handball performed by eight male varsity students. Each subject performed 15 European handball throws per min on a 6-min test. Tests were performed at ball velocities of 40, 50, 60, 70, 80 and/or 100 percent of maximal ball velocity of each subject. Ball velocity was measured using CdS photocell system and the external work was calculated. Expired gas was collected using the Douglas bag method and gas samples were analyzed using the Scholander technique. (Table 1) The mechanical efficiency was calculated with the formula of Gaesser et al. (1975). The mechanical efficiency of all subjects showed a convex quadratic curve. (Figure 1) The highest mean values of mechanical efficiency were 3.9% for the skilled subjects and 3.3% for the unskilled subjects. The difference between these two groups was found to be significant at 0.05 level. Furthermore, the highest skilled subject S.S. showed the highest mechanical efficiency. This occurred at 73 percent of his maximal ball velocity and was 4.2%.

Table 1 Ball velocity, % of max speed, work and O_2 uptake in TEST I, II, III, IV, V and VI.

TEST		Ball velocity (m/sec) Mean	S.D.	% of max speed (%) Mean	S.D.	Work (kgm/min) Mean	S.D.	O_2 uptake (l/min) Mean	S.D.
I	(skilled)	7.65	0.68	42.12	3.33	20.01	3.08	0.62	0.05
	(unskilled)	7.11	0.16	42.17	1.71	17.26	0.74	0.69	0.03
II	(skilled)	9.69	1.04	53.48	6.67	32.35	7.13	0.72	0.14
III	(skilled)	11.54	0.83	68.63	11.73	45.65	6.61	0.88	0.12
	(unskilled)	10.23	0.08	60.75	3.21	36.03	0.94	0.91	0.07
IV	(skilled)	13.54	1.46	74.56	7.47	62.57	14.61	1.08	0.29
V	(skilled)	16.10	1.29	88.75	7.39	88.82	14.58	1.60	0.42
	(unskilled)	13.15	1.51	77.53	4.05	59.72	13.55	1.15	0.13
VI	(skilled)	18.16	0.74	100.00	—	112.79	9.42	2.08	0.12
	(unskilled)	16.91	1.06	100.00	—	95.86	11.34	2.49	0.06

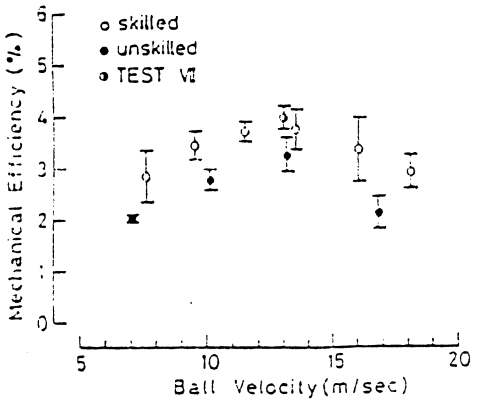

Figure 1 Relationship between ball velocity and mechanical efficiency for skilled and unskilled subjects.

[1]This study was supported by Kanazawa University Research Funds and conducted in Biomechanics Laboratory with the assistance of its members. We would like to thank Mr. Tetsu Nakamura for his considerable technical skill.

[2]Hiroh Yamamoto is a visiting Professor from Kanazawa University, Dept. of Physical Education, Kanazawa, Japan, to Washington State University, Dept. of Physical Education for Women, Pullman, Washington, during the academic year 1982-83.

Design Analysis of The Biomechanical Ankle Platform System

Gary W. Gray, PT, ATC Director, Paramedical Associates Sports Medicine, Toledo, Ohio

The Biomechanical Ankle Platform System is a rehabilitation and conditioning tool for the ankle and lower extremity. The shape and design of the platform is a culmination of an indepth analysis and functional understanding of the biomechanics of the foot, ankle and lower leg. This analysis begins with the documentation of orientation axes within the planes of the body, along with the biomechanical axes that can be transposed on the transverse plane. The range of motion of the components of pronation and supination are then utilized to calculate the exact distances from an axis of rotation for each of these motions. Specific vectors which designate a direction which is perpendicular to the axis of motion, and a distance which correlates to the range of motion, are then calculated trigometrically. The infinite number of other motions that are possible between these vectors along with their ranges, are calculated geometrically and consistent with the biomechanics of motion and function with the use of accelerating and decelerating curves. The resultant shape and design of the platform, therefore, is consistent with the motions that occur, in the direction they occur, along the axis they occur and within the ranges they occur at the foot, ankle and lower leg. When the foot is properly placed on the platform and the platform rotates about a hemispherical attachment on its peripheral edge, biomechanical consistent ranges of motions are produced. Dependent upon the size of the hemispherical attachment, a specific percentage of proportional motions of dorsiflexion, eversion and abduction as components of pronation and plantar flexion, inversion and adduction as components of supination will occur. It is the specific shape and design of the platform that allows exacting control of biomechanically consistent motions of the foot, ankle and lower leg in a weight bearing position. The development of the system also incorporates a functional understanding of the kinesiology associated with the myofascial and tendenous structures during weight bearing in static and dynamic function along with neurological consideration specific to proprioceptive stimulation. The presentation includes a review of the biomechanics of the foot, ankle and lower leg, the development and analysis of the shape and design of the platform along with a description of the protocol parameters for clinical use of The Biomechanical Ankle Platform System as a rehabilitation and conditioning tool.

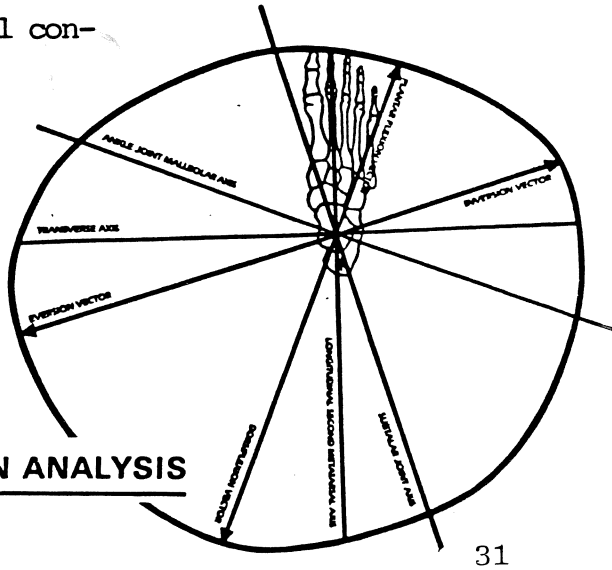

BIOMECHANICAL DESIGN ANALYSIS

FATIGUE PERFORMANCE OF HOFFMANN-VIDAL EXTERNAL FIXATOR

R. Shiba, E. Y. Chao, R. Kasman, and M. Cabanela

Biomechanics Lab, Mayo Clinic/Mayo Foundation
Rochester, MN 55905

INTRODUCTION The joints of a Hoffmann-Vidal external fixator may become loose as they are subjected to high repetitive loads. However, there are no guidelines for retightening. The question concerning reusability of the Hoffmann-Vidal frame has also been widely discussed, but no definite recommendation can be made based on scientific data. The present study was designed to investigate the change of frame stiffness and fatigue life of the components in a Hoffmann-Vidal quadrilateral fixator. Recommendations for sequential application of the same device on a number of patients were made based on the test results.

MATERIALS AND METHODS A standard Hoffmann-Vidal quadrilateral tibial frame with ten smooth 4.75 mm titanium rods was applied to a reproducible synthetic bone model. No contact was allowed at the fracture site. The torsional stiffness of the articulation couplings and the universal ball joints was tested as a function of the tightening torque of each screw. Each screw on the frame was tightened to 11.3 Nm using an instrumented torque wrench. The loosening torque of each screw was measured before and after the fatigue test. The ends of the bone models were fixed in an MTS material testing machine in specially designed jigs. A cyclic axial compressive load of 890 N was applied at a frequency of 5 Hz. Each test was run for 2.5 million cycles. Four frames with unknown histories and four new frames were tested. Two of the new frames were tested further, to a total of 5 million cycles. Each component of the frame was rigidly clamped in a vise and a tightening torque of 11.3 Nm was applied to its fixation screws. The loosening torque was measured after each tightening. This procedure was repeated 400 times or until the screw failed through fracture.

RESULTS Failures were found at the base of the pin fixation bracket post. They can be classified into 3 types: complete post fracture, incomplete post fracture, and loosening of the post. Only complete fractures of the post caused a significant reduction of frame stiffness. Strength and loosening torque were proportional to the initial tightening torque for both the universal ball joint and articulation coupling. The mean reduction of screw fixation strength was 16% after 2.5 million cycles. As a result of repeated tightening, two retaining screws from three universal ball joints were severely deformed and the threads flattened. Two fixation screws on the pin bracket and two square-headed screws on the adjustable connecting rods fractured at the 5th to 6th tightening sequence. Significant wear debris were observed during repeated tightening of the articulation coupling. No gross material defects were observed on the fracture surfaces of the failed components.

DISCUSSION The Hoffmann-Vidal external fixation apparatus may be safely used for four to five sequential applications provided that all critical components be carefully inspected and the fixation screws replaced after each application. The screws should be tightened appropriately using only the T-wrench in order to prevent overloading. These screws should be retightened periodically to maintain a constant joint fixation strength. A few design modifications can be incorporated to minimize the screw and post fractures and to avoid the wear problem after repeated tightening of the screws.

AN EVALUATION OF VARIABLES WHICH ALTER THE MECHANICAL BEHAVIOR OF FIXATOR FRAMES

Fred Behrens, M.D., and Wesley D. Johnson, M.M.E.

Department of Orthopaedic Surgery
St. Paul-Ramsey Medical Center, St. Paul
MMC Biomechanics Laboratory
University of Minnesota, Minneapolis

The clinical limitations of bilateral fixator frames which routinely use transfixion pins and bilateral longitudinal rods for the immobilization of severe skeletal injuries have recently drawn attention to unilateral fixator configurations. These frames occupy a cross-sectional area of less than 90^{o} and can be applied to the anteromedial aspect of the leg without jeopardizing neurovascular structures and musculotendinous units. While these frames are clinically attractive, little is presently known about their mechanical properties. It was the purpose of this study to examine experimentally how such structural variables as the number of pin planes, the spread between the pins, the bone-rod distance, and selective pin loosening would influence the behavior of these frames.

Using components of the AO/ASIF tubular fixator, a number of bilateral and unilateral frames were erected on a model bone and their ability to resist sagittal bending moments, frontal bending moments, and compressive loads was determined using a materials testing machine.

The results from these examinations allowed the following conclusions:

1. Unilateral frames can be as effective in resisting bending moments and compressive loads as the traditional bilateral frames.

2. The following measures are most effective in increasing the resistance to the three tested loading modes.
   AP bending: Adding a second anterior rod.
   Transverse bending: Adding a second half frame in the transverse plane.
   Compression: Adding a second rod and decreasing the bone-rod distance.

3. A gradual and predictable decrease of frame rigidity in all three loading modes can be achieved by the sequential dismantling of unilateral frames. With this method, increasing loads can be transmitted across the fracture site in the bony healing period.

Supported by a grant from the St. Paul-Ramsey Medical Education & Research Foundation (#8327).

BONE MINERAL CONTENT IN THE FIRST METATARSAL: NORMS FOR WOMEN

R.B. Martin and R.A. Yeater
West Virginia University, Morgantown, WV 26506

The most commonly used site for measuring bone mineral content (BMC) by photon absorptiometry is in the distal shaft of the radius. Although some work has been done with the os calsis, an equivalent lower extremity site has not been developed. Such a site would have the advantage of being sensitive to weight-bearing exercise, an important determinant of bone mass and strength in the lower extremities and spine. We have therefore developed a site for photon absorptiometry in the shaft of the first metatarsal. This paper reports normal values for this site in women as a function of age and compares age-related changes to those seen in the radius.

The new site is located by measuring the distance from the back of the heel to the metatarsal-phalangeal joint, and marking a point on the dorsal aspect of the foot that is 90% of this distance. This location falls near the middle of the first metatarsal's diaphysis. Using the non-dominant foot, this site was scanned four times in the mediolateral direction using a Norland-Cameron Bone Mineral Analyzer, and the resulting BMC and bone width (BW) values were averaged. A similar procedure was followed at the conventional site in the distal shaft of the non-dominant radius. In addition, the cross-sectional moment of inertia (CSMI) of the bone at each site was estimated from the BMC and BW data using a tubular bone model. This estimate has been shown to be highly correlated (r = .98) with the value digitized from histologic cross-sections of the radius.

The mean BMC of the metatarsal was somewhat less than that of the radius in every age group; maximal values were 0.91 and 0.88 gm/cm in the radius and metatarsal, respectively. As in previous studies, the BMC of the radius declined significantly after age 50. The BMC of the metatarsal also decreased significantly with age, but in this case the change was less rapid and appeared to begin a decade later than that of the radius. The metatarsal is a wider bone at the scan site, but both bones increase in width as women enter the 60's and 70's.

The estimated CSMI of the radius did not decline significantly with age. This result is in concert with our previous work showing that the torsional rigidity of the radius scan site does not decrease with age. Conversely, the metatarsal CSMI decreased 30% between the fourth and eighth decades.

Younger women exhibited a significant correlation between radius and metatarsal BMC, but older women did not. This fact may be related to age-related changes in activity patterns which differentially affect the upper and lower extremities. It is anticipated that future studies will utilize the metatarsal site to clarify the combined effects of age and exercise on the skeleton. We are presently developing male norms for the metatarsal site.

CHARACTERIZATION OF JOINT MOMENT PATTERNS AS A FUNCTION OF WALKING SPEED

Schein, S.S., Andriacchi, T.P. and Strickland, A.B.
Department of Orthopedic Surgery
Rush-Presbyterian-St. Luke's Medical Center
1753 West Congress Parkway
Chicago, IL 60612

A knowledge of joint moments, as a measure of function during walking, can be an important tool both for understanding normal gait and for the evaluation of abnormal gait. The purpose of this study was to classify normal patterns and magnitudes of joint moments at the hip, knee and ankle and to determine the influence of walking speed on these parameters.

The moments acting at the major joints of the leg were analyzed using an optoelectronic system, force platform, 10 meter walkway and minicomputer. Three hundred and sixteen stride cycles from 29 subjects were analyzed. The moment pattern at the hip joint was the most reproducible of the three major joints in the leg with 99% of all observations demonstrating the same pattern, independent of walking speed. The knee joint had three distinct flexion-extension moment patterns at slower speeds. However, at faster speeds, this variability diminished with 86% of all observations having the same pattern. The greatest variability in moment patterns was found in the ankle joint with two distinct flexion-extension, three inversion-eversion, and three internal-external rotation patterns. For each of the three joints, the magnitude of the flexion-extension moments were found to increase with walking speed.

The findings of this study indicate that it is possible to characterize moment patterns for normal gait at three different walking speeds which can serve as a basis for the clinical evaluation of abnormal gait.

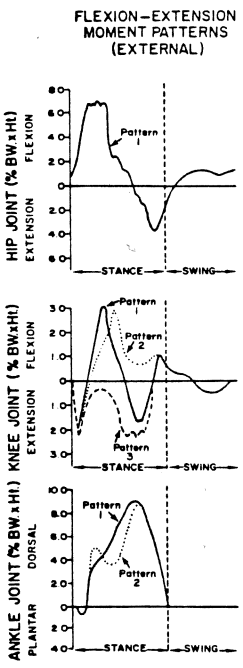

PATTERN FREQUENCY
PERCENT TOTAL OBSERVATIONS

Speed	Pattern	All Subject	Male	Female
Slow	1	99	98	100
	Other	1	2	0
Normal	1	99	98	100
		1	2	2
Fast	1	100	100	100
	Other	1	0	0
Slow	1	60	62	58
	2	13	12	13
	3	27	26	29
	Other	0	0	0
Normal	1	79	84	75
	2	5	6	5
	3	16	10	20
	Other	0	0	0
Fast	1	86	81	91
	2	9	11	7
	3	5	8	2
	Other	0	0	0
Slow	1	90	88	92
	2	10	12	8
	Other	0	0	0
Normal	1	77	70	84
	2	23	30	16
	Other	0	0	0
Fast	1	51	49	53
	2	49	31	47
	Other	0	0	0

FIGURE 1 - An illustration of the most frequently occuring patterns of flexion-extension moments at the hip, knee, and ankle joints. The table gives the percentage out of 316 stride cycles that each pattern occurs, at 3 different walking speeds.

THREE-DIMENSIONAL LOWER EXTREMITY JOINT FORCES AND TORQUES IN WALKING

M. SABRI EKEN AND MAX DONATH

Department of Mechanical Engineering
University of Minnesota
Minneapolis, Minnesota 55455

INTRODUCTION

In a quantitative study of biped gait, the important moving unit is not only the skeletal structure that supports the surrounding tissues but also the total mass of the body segments that rotate about the respective joint axes. The scope of this study is the inverse dynamics problem. In this problem, the motion of the body is known at the joints, but the applied forces and moments are to be determined.

A mathematical model is proposed to approximate the human musculo-skeletal system by a spatial linkage system. The objective of the mathematical modelling is to describe the joint's angular motion and relate them to the overall translatory process of locomotion. Such a mechanical description does not incorporate the individual contributions of the muscles. The complexity of the model developed depends on the assumptions made about the gait and the degrees of freedom allowed in the model. Important objectives of such a model (at a given speed and ground profile) would be to insure:

i) support of the body
ii) maintenance of the balance in the upright position
iii) synchronization of the motion of the two extremities to achieve coordinate phasic and temporal paterns
iv) forward progression

Clinicians, such as J. B. DeC. Saunders, et al., (1) and Elftman (2), have for some time emphasized the importance of the three-dimensional nature of gait. The motivation for this study was to see if a simplified model that included three-dimensionality could be useful in predicting the overall forces and moments in the joints.

MODEL

The proposed model is formed by a seven-link chain composed of lower limbs (each three segments: the foot, shank, and thigh) and the head, arms, and trunk (HAT) lumped into a single segment. This last assumption neglects the independent motion of the four elements (head, two arms, and trunk). The most significant of these is the rotation of the trunk with respect to the pelvis and the rotation of the head about the vertical axis, which is accompanied by swinging of the arms. The swinging of the arms and rotation of the trunk tend to counterbalance an opposite rotation of the pelvis as the legs swing forward. By not considering the arm swing, the calculated moment about the limb's major axis at the hip joint will be higher than if the arm swing was included. Although the HAT is rather massive, representing 67.8% of the body weight, the trunk rotation and swinging of the arms are assumed to be of small magnitude for lower walking speeds, and the resulting error turns out not to be significant in our case.

The foot and the toe are considered as a single segment. The application point of the reaction forces and the moments are predicted to move at a constant rate from the heel to the ball of the foot during the deploy phase. The toe is assumed not to carry a load at any instant of the double step period.

METHOD

The Whole Body Method is used to solve the mathematical model, that is, the computation of the forces and moments are initiated by considering the swinging foot (no floor contact, zero reaction force) and proceeding segment by segment until the ground reactions under the loadbearing foot are calculated. For the double support phase, the calculations start from the deploying foot. Euler angles are used to determine the position and orientation of the segments in space, and to calculate their angular accelerations. Newton-Euler Equations are used to solve for the system dynamics.

RESULTS

Together with the joint forces and moments, the components of the ground reactions were also calculated at one hundred intervals per gait cycle. The results included vertical forces, the fore-aft shear, and the medio-lateral shear on the ground; the ground reaction moments in the sagittal, frontal, and transversal planes; the forces and moments at the ankle; and the reactions at the hip.

CONCLUSIONS

The results were compared qualitatively with data presented in the literature. Given the assmptions that were made vis-a-vis the determination of mass, the logitudinal, and transverse lengths, the center of gravity of the segments and the moments of inertia based on Dempster (3) and others, and the relative simplicity of the model, the results were surprisingly good. This speaks to the relative insensitivity of the results to inaccuracies in the anthropomorphic data. Further detail on the assumptions made, the calculated results, and conclusions are presented by Eken (4).

BIBLIOGRAPHY

1. Saunders, J. B. DeC., V. T. Inman, and H. D. Eberhart. "The Major determinants in Moral and l'athological Gait." J. Bone and Joint Surgery, 35A: 543-558, 1953.
2. Elftmann, H. "The Basic Pattern of Human Locomotion. Annals of the NY Academy of Sciences 51(7), January 31, 1951.
3. Dempster, W. F. "Space Requirements of the Seated Operator." U.S. Air Force Report No. WADS 55-159. 1955.
4. Eken, M. Sabri. A Three-Dimensional Dynamic Model for Walking. S. M. Thesis. Department of Mechanical Engineering, University of Minnesota. December, 1981.

AN ANALYSIS OF STAIRCLIMBING IN ANTERIOR CRUCIATE DEFICIENT SUJBECTS

Belcher, M.K., Reider, B., and Andriacchi, T.P.*
Department of Surgery, University of Chicago, Chicago, IL
*Department of Orthopedic Surgery, Rush-Presbyterian-St. Luke's Medical Center, Chicago, IL

The importance of the anterior cruciate ligament (ACL) in maintaining knee stability during vigorous sports activities is widely accepted. Less widely accepted is the importance of the ACL in maintaining normal knee function during less stressful activities of ordinary life. A functional analysis of stairclimbing in ACL deficient subjects demonstrated significant deviations from normal limb segment angles, flexion-extension moment patterns, and maximum stance phase moments.

Stairclimbing function was evaluated in ten normal and ten ACL deficient males between the ages of twenty and thirty-two years. A two-camera optoelectronic system was used for three-dimensional motion analysis. A three-step staircase with a height of 21 cm and a slope of 38 degrees was instrumented with a multicomponent force platform for measurement of foot-floor and foot-step reaction force. Data was collected bilaterally from both groups. As the subjects ascended, measurements were made from foot-strike on the first step to foot-strike on the third step, and from foot-strike on the floor to foot-strike on the second step. During descent, measurements were made from toe-off from the third step to toe-off from the first step, and from toe-off from the second step to toe-off from the floor. Relative segmental angles were measured and forces and moments acting at the hip, knee, and ankle were calculated. Moment magnitudes were normalized for height and weight.

Peak stance phase knee flexion angles were greater in ACL deficient subjects during ascent from step to step and during descent from step to step by more than 20 degrees. Maximum stance phase knee flexion moments were increased during ascent from stair to stair by two percent of bodyweight times height. Maximum stance phase knee extension moments were decreased by one and one-half percent of bodyweight times height during descent from stair to floor, and decreased by two percent bodyweight times height during ascent from floor to step. These differences were significant at 95% probability. Moment patterns in ACL deficient subjects differed from those previously described for stairclimbing in normal subjects.

The increased flexion moments, decreased extension moments, and increased knee flexion angles found in data from ACL deficient subjects suggest alterations in the mechanics of the knee during stairclimbing. These findings imply that an intact ACL is needed for normal knee function during stairclimbing.

PATTERN RECOGNITION FEATURES FOR IDENTIFYING GAIT DISABILITY BASED ON THE ANGLE-ANGLE DIAGRAM

by

JANE MACFARLANE AND MAX DONATH

Department of Mechanical Engineering
University of Minnesota
Minneapolis, MN 55455

In the last few decades, gait laboratories around the world have provided considerable valuable parametric information on the biomechanical phenomena involved in walking. Visual observations by clinicians have been the traditional mode for the assessment of pathological gait. However, it has been a long standing desire to come up with quantitative object measures which integrate the data in a clinically useful manner, isolating out the factors contributing to the pathology, serving as a mechanism for tracking patients, and as a means for comparing the efficacies of various therapeutic procedures.

One pattern recognition based approach has been the development of multivariate standard deviations measured from the discriminant boundary separating normal and abnormal gait data in a multi-dimensional feature space (1,2). Angle-angle diagrams have, for some time, been proposed as a mechanism for visually describing the interrelationships between the trajectories of two joints, typically in the lower extremity. Hershler and Milner (2,3) have proposed the use of three features--area, perimeter, and the nondimensional ratio of perimeter to the square root of the area--to analyze the angle-angle diagram of knee versus hip flexion. Thus, these three measures serve to characterize the overall shape of the angle-angle diagram. Since the shape of the angle-angle diagram varies with the pathology, the three features do provide some measure of the shape change. However, one must develop a mapping of how changes in the three feature set can be used to identify improvement or deterioration in the overall gait and, furthermore, isolate where in the gait cycle improvements must take place.

A "deviation from normal" measure based on the angle-angle diagram is proposed herein. Consider the knee angle-hip angle diagram as simply a two feature set plotted with time as the independent parameter. Since gait is cyclic in time, this feature set forms a closed figure. Given a sampling of normal curves, a mean curve is determined. A boundary around the mean curve is defined based on the maximum deviation any of the normal curves makes from the mean. This boundary defines the maximum tolerable distance from the mean that a point representing the angle coordinate pair can be without being considered an abnormal point on the angle-angle trajectory. If the patient's gait under consideration deviates outside the boundary area, points on the curve are considered abnormal and the distance between the point and the boundary is computed.

This distance metric represents the "deviation from normal" and can be plotted versus percent of gait cycle. Some interesting patterns in the results appear using data from the Hershler/Milner work (3,4) which can be used to identify the pathology and isolate the contributing factor. Furthermore, the area under this deviation curve provides an integrative measure of gait abnormality.

REFERENCES

1. Donath, M. "Human Gait Pattern Recognition for Evaluation, Diagnosis, and Control." Ph.D. Thesis. Mechanical Engineering Department. M.I.T. 1978.
2. Donath, M. and W. C. Flowers. "Human Gait Evaluation by Pattern Recognition." Proceedings of the 25th Annual Meeting of the Orthopaedic Research Society. San Francisco. 1979. Appears in Orthopaedic Transactions, May 1979.
3. Hershler, C. and M. Milner. "Angle-Angle Diagrams in the Assessment of Locomotion." American Journal of Physical Medicine, 59(3). June, 1980.
4. Hershler, C. and M. Milner. "Angle-Angle Diagrams in Above-Knee Amputee and Cerebral Palsy Gait." American Journal of Physical Medicine, 59(4). August, 1980.

IN VIVO MEASUREMENT OF SPINAL COLUMN VIBRATIONS

M. Panjabi (Department of Surgery, Yale Medical School, New Haven, CT 06510, USA),
G. Andersson, L. Jörneus, E. Hult, L. Mattsson

Department of Orthopaedics, Sahlgren Hospital, Gothenburg, Sweden

Throughout life, our bodies are exposed to a wide range of shock loads and vibrations. Forced vibrations is a well-known environmental health problem. Recent epidemiological studies indicate higher risk factors for persons exposed to vibrations. In vivo studies that measure transmission of whole body vibrations through the spine can provide vital information. Most previous studies have measured this transmission property of the spine in an indirect manner, for example by placing accelerometers on the skin, in the mouth or on the head. The experimental study presented here measures the actual in vivo response of a given lumbar vertebra when the whole body is subjected to a given vibration input.

Materials and Methods - The material consisted of healthy volunteers. The vibration exposure was given to the person in a sitting posture. A specially-designed machine that produced pure sinusoidal vertical vibration was utilized. The available electrohydraulic types of machines were found to be unsuitable, since they could not produce a clean, pure, sinusoidal input. Two acceleration amplitudes were used: 0.1 and 0.3 times the acceleration due to gravity (1 and 3 m/s.s). The frequency input ranged from 2 to 15 hertz.

Vibration along the spine was measured at three different points: in the sacrum and on two vertebral levels in the lumbar spine. A threaded K-wire 2.4 mm in diameter was threaded about 10 mm into the sacrum and the spinous processes of the two vertebrae. They were oriented to lie in the mid-sagittal plane. A single-axis acceleration transducer was rigidly fixed to the sacrum pin while a specially-designed three-accelerometer transducer (PAT) was placed on the pins of the vertebrae. The PAT was capable of measuring complete acceleration of the vertebrae in the sagittal plane. Thus, by using a method in which a three-accelerometer transducer was directly attached to the vertebrae by a rigid pin, it was possible for the first time to measure the dynamics of a vertebra in vivo.

Data Analysis - The six signals from the two PATs, one from sacrum accelerometer and one from an accelerometer placed on the vibrating seat were stored on magnetic tape and later processed in a minicomputer. Since the body vibration was stationary, the R.M.S. value of each signal was used in the analysis. The output for each PAT was transformed to its corresponding vertebral body with the help of an x-ray taken on the subject. The transformation provided translation acceleration in the disc plane and perpendicular to the vertebral axis (Tz) and a rotatory acceleration of the vertebral body in the sagittal plane (Rx). Dividing these accelerations by the input acceleration as measured by the seat transducer, the transfer functions of the spinal column were computed. These were plotted as a function of the frequency.

Results - The graphs show that the frequency characteristics for the same lumbar vertebra differ quite dramatically in different directions. The transfer function for the axial translation increases from a value of about 1 at 2 hertz to a peak of 1.5 at about 4 to 5 hertz, then decreases to about .5 between 9 and 14 hertz. The anterior-posterior acceleration of the vertebra, however, seems to increase continuously from 2 to 15 hertz. Finally, the rotatory acceleration of the vertebra seems to change a little, reaching a maximum at around 8 hertz.

The results indicate that the vibration motion pattern along the spine is frequency-dependent. Further, the vertebral motion, as excited by a simple sinusoidal vertical acceleration, is complex. The vertebra not only accelerates in the direction of the input, but also perpendicular to it and in addition has a rotatory component. We believe that studies of the type presented here will provide a better understanding of the dynamic behavior of the spinal column.

Acknowledgements: Research supported by Swedish National Work Environment Fund, and N.I.H. grants NS-10174 and K04 AM00299.

EVALUATION OF SPINAL DEFORMITY BY MEANS OF INTRINSIC CURVATURE AND TORSION

Dansereau, J., Allard, P., Thiry, P.S., Raso, J.V., Duhaime, M.
Department of Mechanical Engineering, Ecole Polytechnique, Montreal
Pediatric Research Center, Sainte-Justine Hospital, Montreal
School of Physical and Occupational Therapy, McGill University, Montreal
Glenrose Hospital, Edmonton, Canada

INTRODUCTION: Scoliosis is routinely assessed at Sainte-Justine Hospital by means of a tridimensional reconstruction model of the spine based on the centroid location of the thoraco-lumbar segment vertebrae obtained from standardized radiographs (McNeice et al., 1975). This reconstruction based on cubic spline functions computes spatial parameters such as the projected surface area index and the kypho-scoliotic index which give valuable information on the spinal deformity. This method has some limitations in particular to account precisely for the torsion encountered in Friedreich's Ataxia (Allard et al., 1982). Hierholzer and Lüxmann (1982) have suggested the use of invariant shape parameters to describe the scoliotic spine. This paper presents a similar approach where a more thorough description of the shape of the spine curve is obtained by means of its intrinsic curvature and torsion.

DEFINITION OF THE INTRINSIC CURVE PARAMETERS: The basic equations to determine the intrinsic curvature $\kappa(s)$ and torsion $\tau(s)$ of a spatial curve, function of s, its arc length parameter, are deduced from the well known Frenet formulas:

$$\frac{d\vec{T}(s)}{ds} = \kappa(s)\,\vec{N}(s), \qquad \frac{d\vec{B}(s)}{ds} = -\tau(s)\,\vec{N}(s)$$

which are expressed in terms of the Frenet frame field, composed of $\vec{T}(s)$, unit tangent vector, $\vec{N}(s)$, unit principal normal vector and $\vec{B}(s)$, unit binormal vector (O'Neill, 1966).

METHODS: To obtain the numerical values of $\kappa(s)$ and $\tau(s)$, it is essential to know the first to the third derivative of the spine curve at each point. The derivatives are calculated by an interpolation method using quintic spline functions.

RESULTS: For a Friedreich ataxia patient, an attempt was made to extract, from these intrinsic parameters the most diagnostically relevant information: the maximum curvature (κ_{max}), the maximum curvature of the antero-posterior plane projection (κ_{APmax}), the maximum curvature of the lateral plane projection (κ_{LATmax}) and the maximum torsion difference in the scoliotic region ($\Delta\tau_{max}$). The most interesting observations shown in Table I are that:

i) κ_{APmax} has an evolution which can be put in correspondence with the Cobb angle,
ii) κ_{max} represents not only the extent of scoliosis but also of kyphosis,
iii) $\Delta\tau_{max}$ measured from T4 to T8 shows a dramatic increase at the 2nd and 3rd visit.

This analytical technique represents an improvement in the spatial shape description of the scoliotic spine.

ACKNOWLEDGEMENTS: This research was funded by the Canadian Friedreich Ataxia Association and by the Institut de Recherche en Santé et en Sécurité du Travail du Québec.

REFERENCES:

-Allard, P. et al. (1982). Can. Journal of Neurological Sc., 9:105-111.
-Hierholzer, E. and Luxmann, G. (1982). J. Biomech., 15:583-598.
-McNeice, G., Koreska, J. and Raso, J. (1975). ASME Winter Annual Meeting, Houston, 76-86.
-O'Neill, B. (1966). Elementary Differential Geometry. Academic Press, New York.

Table I: Clinical data obtained on the spine curve reconstruction for a Friedreich ataxia patient (C.G.) over a 12-month period.

VISIT	AGE (years)	COBB ANGLE (°)	κ_{AP}^{max} (m^{-1})	κ_{LAT}^{max} (m^{-1})	κ_{max} (m^{-1})	$\Delta\tau_{max}$ (m^{-1})
1	16	24	6.7	10.1	10.0	6.6
11	16½	33	7.1	8.1	8.1	24.5
111	17	38	11.7	7.1	11.5	51.8

THE STRENGTH OF SPINAL LIGAMENTS

J.B. Myklebust, F. Pintar, D. Maiman, and A. Sances, Jr.
Department of Neurosurgery, Medical College of Wisconsin, and
Wood V.A. Medical Center, Milwaukee, Wisconsin 53226

Tkaczuk reported failure loads of 200-640 N for the anterior longitudinal ligament and 100-250 N for the posterior longitudinal ligaments in the lumbar spine of the human cadaver.[4] Similar studies were reported in the nonhuman primate.[1] Studies in the fresh human cadaver in our laboratory suggest that in axial tension the anterior complex at cervical levels 4-6 can withstand approximately 1000-1300 N, while the posterior complex fails at 450-675 N. Isolated cervical spines with all ligaments intact failed in tension at 1200-2200 N. For comparison, the isolated ligamentous cervical spine of the rhesus monkey failed at 325-618 N with all ligaments intact. The anterior complex failed at 195 N while the posterior complex required 100 N.[2,3] Additional studies were conducted in isolated spines of fresh human cadavers and macaque monkeys.

METHODS & RESULTS

The isolated ligamentous spines of 10 fresh male humans, ranging in age from 43-65 were used. For comparison, 2 rhesus (macaca mulatta) and 2 stumptail (macaca arctoides) monkeys were also isolated. In all cases, the tissues were maintained at 2° C and wrapped in towels soaked in Ringer's solution until the experiment (1-3 days). At each vertebral level, all ligaments except the one under study were sectioned under a dissecting microscope. The vertebral bodies above and below the ligament were fixed in a frame using 5 Steinman pins. The ligaments were pulled in direct axial tension at rates of 1-100 cm/sec using an MTS electrohydraulic system. The anterior and posterior longitudinal ligaments, joint capsules, interspinous ligaments, and ligamentum flavum were studied.

In the humans, the strongest ligaments were observed at atlanto-occipital and lumbar levels. The anterior longitudinal ligament and the joint capsules demonstrated failure loads of 50-500 Newtons, with the lowest values in the mid cervical spine. The interspinous ligament ranged from 30-150 N, with the highest values observed at lumbar levels. The posterior longitudinal ligament failed at loads approximately 1/3 to 1/2 of those of the anterior longitudinal ligament. Similarly, the monkey ligaments were strongest at upper cervical and lumbar levels. The anterior longitudinal ligament and joint capsules were consistently the strongest. The interspinous and posterior longitudinal ligaments were the weakest. For the rhesus, the observed failure loads were 2-5 times less than for the humans. The anterior and posterior longitudinal and interspinous ligaments of the stumptail monkeys were approximately the same as those of the rhesus. However, the ligamentum flavum and joint capsules had higher failure loads in the stumptail, probably reflecting a greater cross sectional area.

REFERENCES

1. Little RW, et al: Mechanical properties of spinal ligaments for rhesus monkey, baboon and chimpanzee, Report No. AFAMRL-TR-81-40, Air Force Aerospace Medical Reseach Laboratory, Wright-Patterson Air Force Base, June, 1981, 39 pp.
2. Sances A Jr, et al: The biomechanics of spinal injuries, CRC Crit Rev Bioeng (In press)
3. Sances A Jr, et al: Experimental studies of brain and neck injury. Proc 25th Stapp Car Crash Conf, Society of Automotive Engineers, Warrendale, PA, 1981, pp. 149-194.
4. Tkaczuk H: Tensile properties of human lumbar longitudinal ligaments, Acta Orthop Scand Suppl, 115:1-69, 1968.

Supported in part by ONR Contract No. N00014-77-C-0749

Analysis of Loads on Lumbar Trunk during Hammer Throw

Inseong Hwang (Yonsei University, Dept. of Physical Education, Seoul, Korea)
Marlene Adrian (Washington State University, Dept. of Physical Education, Pullman, Washington)

Compressive, shear forces and muscle recruiting pattern on L3 level were predicted using the biomechanical model of Schultz, et al.(1982) for an hammer throw. The kinematic and kinetic data were obtained from the overhead and side view high speed cameras and strain gage dynamometer system which read the tensional force on the hammer wire. The net forces and the net moments in three dimensions were calculated with an assumption of quasi-static for each succesive 5.9 msec. intervals of the hammer throw using equilibrium equations. The 22 muscles L3 trunk cross-sectional model was used to predict the compressive forces using linear programming assuming that antagonistic activity in the trunk muscles would be as small as possible. The shear forces were calculated from the muscle forces and the net forces

The maximum muscle contraction intensity was 1104 KPa. The maximum compression force was 9331 N. The peak compression force during each revolution occurred at the beginning of the ascending phase. The maximum shear forces in anteroposterior and lateral directions were 1670 N and 679 N respectively.

SHEAR FORCES IN X Y DIRECTION ON L3

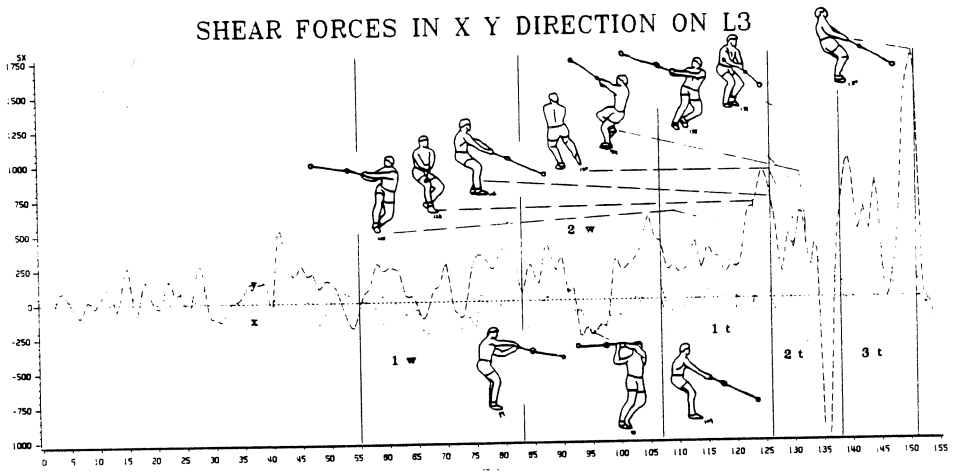

COMPRESSION FORCES ON L3 DURING HAMMER THROW

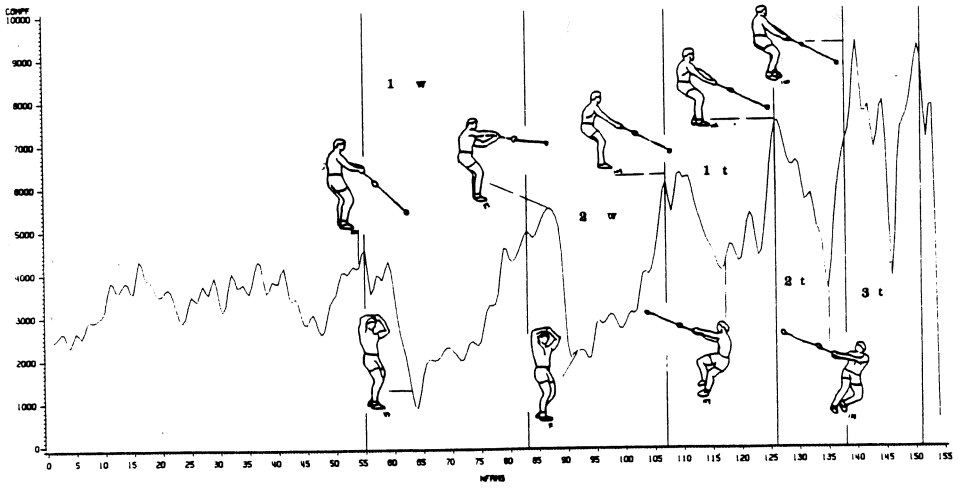

SHEARING OF MUCUS BY CILIA AS INDICATED BY VELOCITY PROFILES IN MUCOCILIARY FLOWS (H.Winet†*,G.T.Yates*,T.Y.Wu* and J. Head†, *California Institute of Technology and †University of Southern California School of Medicine)

Flow velocity profiles within mucus of a mucociliary system have been obtained in order to shed light on the need for ciliary penetration to move mucus. The technique essentially utilizes cilia as rheometers. The profiles were obtained for mucus thicknesses ranging from about 400 to 700 μm and bulk viscosity about 27 cp at 1 sec^{-1} shear rate. Fluorescent microspheres served as flow tracers and were mixed with the mucus before it was deposited on an excised rectangle of frog palate ciliated epithelium. Profile layers were determined by focusing with a microscope via a calibrated fine adjustment. Velocities were computed from cine and video recordings of the particle motions in each vertical mucus layer. Flow in the mucus blob was compared with a control Newtonian solution in which the mucus-depleted epithelium was completely submerged. By utilizing the F-ratio statistic to determine goodness-of-fit, both linear and quadratic regression lines were evaluated and control data were compared with autologous mucus data. It was found that in spite of the difference in boundary conditions between the two fluid preparations, the two sets of profiles which were normalized to liquid depth H_m and maximum particle velocity U_m were indistinguishable for fluid depths above 60 μm from the mucosa. The near-mucosa profiles, in contrast, were unalike with mucus exhibiting the greater velocity gradient as shown in Figure 1. The linear slope of the velocity profile in the 60 μm region led to the conclusion that ciliary contact with mucus is not necessary for generation of mucus flow provided the ciliary shear is not negated by the observed mucus 'flake' or 'slab' being in simultaneous contact with ciliostatic patches which would act as anchors.

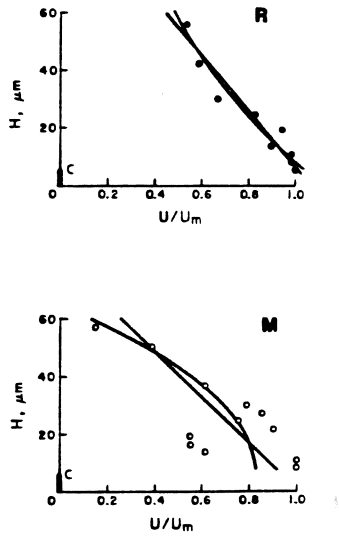

Fig. 1. Lower region velocity profile. U is fluid. particle velocity and H is liquid depth.

Supported by NIH grant HD-51442 and NSF grant CME 77-21236.

STRAIN ENERGY CHARACTERISATION OF HUMAN AORTIC TISSUE IN UNIAXIAL TENSION

K.B.Sahay and Dinesh Mohan
Centre for Biomedical Engineering
Indian Institute of Technology,Delhi,INDIA

Various forms of strain energy functions (or their derivatives) have been proposed to describe Rubber like materials (RLMs) and soft biological tissues (SBTs), but there is little agreement on a suitable form. Nineteen such functions were considered (1) and four selected and examined for SBT characterisation in this study. The purpose of this study was to see which of these four functions most adequately represent human thoracic aortic tissue behaviour at quasi-static strain rates in unaxial tension. Eight curves were selected from an earlier experimental study done by Mohan (2). Curve fitting was done for each one of them using an ICL 2960 computer. The results are shown in Table I. For tissues like human descending thoracic aorta, it appears that the Hart-Smith function and the Veronda and Westmann function are more appropriate than others. Details of the suitability of these functions are discussed in this paper.

Function	Σ^2 Mean	SD
1. Hart-Smith Function $\phi = G \exp [K_1(I_1-3)^2]$, $\Psi = \frac{GK_2}{I_2}$	233	271
2. Mooney Function $\phi = C_1$; $\Psi = C_2$	30110	48713
3. Vernonde and Westmann Function $\phi = A_1 [\exp \{\beta (I_1-3)\}]$; $\Psi = A_2$	265	258
4. Blatz Function $\phi = B \exp [\alpha (I_1-3)]$; $\Psi = 0$	513	339

Table I. Comparsion of the four strain energy functions

($\phi = 2\frac{\partial W}{\partial I_1}$, $\Psi = 2\frac{\partial W}{\partial I_2}$, W = strain energy function

I_1, I_2 are the strain invariants and the rest are constants)

References

1. Sahay,K.B., On the choice of strain energy function for mechanical characterisation of soft biological tissues. (Communicated)

2. Mohan,D., Passive mechanical properties of human aortic tissue, Ph.D Dissertation, the University of Michigan,USA,1976.

FINITE DEFORMATION OF THE LEFT VENTRICLE IN ISOVOLUMIC RELAXATION

Samuel E. Moskowitz
The Hebrew University
Division of Applied Mathematics
Bergmann Building, Givat Ram
Jerusalem 91904, Israel

In isovolumic relaxation of the left ventricle, cavity pressure p_o rapidly falls under biochemical control of the mechanical properties of the inhomogeneous and anisotropic myocardium.

Suppose the ventricle occupies $B \subset V$ a region of euclidean 3-space. It deforms in relaxation according to the mapping $d: B \to d(B)$, such that the jacobian $\det \nabla d > 0$, and d is a smooth homeomorphism.

Let the gradients be represented by $D = \nabla d$ and $U = \nabla u$, where $u(x) = d(x) - x$ is the displacement of a material point originally at $x \in B$. The finite strain tensor is $E = \frac{1}{2}(D^T D - 1) = \frac{1}{2}(U + U^T + U^T U)$ with $D^T D$ the right Cauchy-Green strain tensor. Incompressibility is met by $\det D = 1$.

If X and Y are the spaces of all symmetric and general second order tensors, respectively, $f: X \to X$ is defined by $f(E) = \hat{S}$, while $g: X \to Y$ is given by $g(E) = S$. We take the 6-component vector e formed from the distinct elements of $E = E^T$, transform using $K_x e = \hat{s}$, then construct $\hat{S} = \hat{S}^T$. K_x is a function of the 5 moduli characterizing a transverse isotropic and inhomogeneous myocardium with preferred fiber orientation. The Piola-Kirchhoff stress $S = D\hat{S}$ satisfies $SD^T = DS^T$, hence angular momentum, the principle of frame indifference, the equation of motion $\operatorname{div} S + b = \rho \ddot{u}$ with body force b and mass density ρ, endocardial condition $S(x)\, n(x) = p_o$, $x \in \partial B_o$, epicardial condition $S(x)\, n(x) = p_1$, $x \in \partial B_1$, where p_1 is the pleural-pericardial pressure, and n the unit normal to the surface. The Cauchy stress $T = (\det D)^{-1} SD^T$ is then reckoned relative to the deformed configuration.

The surface $\partial B = \partial B_o \cup \partial B_1$ is assumed regular, and B simply connected by cut C such that $\lim u^+(x) = \lim u^-(x)$, $x \in C$.

A LASER SCANNING SYSTEM FOR TRACKING MOTION IN 3-D SPACE FOR BIOMECHANICAL APPLICATIONS

by

JANE F. MACFARLANE AND MAX DONATH

Department of Mechanical Engineering
University of Minnesota
Minneapolis, Minnesota 55455

INTRODUCTION

The literature abounds with new approaches for measuring motion. Chen (1) and Taylor (2) provide good descriptions of many presently available systems. The need for a low-cost, 3-D, measurement system with good resolution is evident by the numerous measurement systems available. A new approach to the measurement problem is suggested, with the aim of simplicity to achieve low cost but without sacrificing resolution, sampling rate, or versatility.

CONFIGURATION

Three-dimensional position data is determined using a laser scanning system (3). Spatially separated, low power lasers are used to scan the target field. Coverage of the entire field is accomplished by passing each of three lasers through an optical lens arrangement based on a cylindrical lens plus focusing optics, which produces a plane of laser light in 3-D space. This plane of light is then directed at an eight-sided, mirrored scanner rotating at a constant speed of 3600 revolutions per minute. Each scanner is phased so as to allow only one beam of light in the target field at any instant in time. Photodetectors capable of sensing the laser light are attached to moving parts of the target of interest. Since three (x,y,z) locations determine the position and orientation of a rigid body in space, a minimum of three photodetectors must be attached to each limb segment.

The measurement area for the gait analysis is a cube 6 feet x 6 feet x 4 feet centered over a walkway incorporating an instrumented force platform. The subject is asked to walk through the laser scanned volume. The detectors are attached to each limb segment so as to ensure that there is a direct line of sight between the detector and the scanning laser beam.

As the target travels through the scanned volume, the target receivers are triggered by the scanning laser beam. Two fixed reference photodiodes are placed at the perimeter of the field. An electronic pulse is generated each time a photodetector is hit by the moving light. By measuring the elapsed time between pulses from the stationary reference diodes and the moving target, one can derive a measure of the swept angle, given a constant angular velocity for the scanning plane. Using trigonometric relations, the coordinate of the target diode may then be calculated. Figure 1 demonstrates the position of the beams of light from the three lasers as they each hit a specific target detector. Although the three beams are never in the target area at the same time, the intersection of the three beams will identify the target location. The system is capable of generating 480 (x,y,z) points per second per target.

CALIBRATION: TWO-DIMENSIONAL CASE

The (x,y) position data is determined as a function of several system parameters. Therefore, a procedure is required to calibrate the system and obtain the correct system parameters.

For a two-dimensional system, there are four unknowns, the (x,y) locations of two lasers. Thus, four equations are required. Consequently, the calibraiton grid requires five detectors. One detector is used as a reference, and the remaining four detectors are used to generate the four calibration equations. The calibration equations are highly nonlinear functions of the source points. A Newton-Raphson technique for nonlinear systems is used to calculate the solution.

CONCLUSIONS

A two-dimensional prototype has demonstrated that the proposed technique is viable for tracking motion in space. A three-dimensional version is now being built. Consideration of safety vis-a-vis the lasers has been taken into account. The nonlinear effects due to the lens' distortions associated with camera-based techniques have been avoided. Furthermore, there is no upper limit as to the number of targets that can be handled with the same resolution, accuracy, sampling rate, etc.

REFERENCES

1. Chen, H. J. A Minicomputer-Multiple Microprocessor System for Gait Analysis Using Television and Force Place Data. Ph.D. Thesis. Ohio State University. August, 1977.
2. Taylor, K. D., et al. "An Automated Motion Measurement System for Clinical Gait Analysis." Journal of Biomechanics, Vol. 15, pp. 505-516, 1982.
3. Macfarlane, J. A System for Tracking Motion in Three-Dimensional Space. M.S.M.E. Thesis. University of Minnesota. June, 1983.

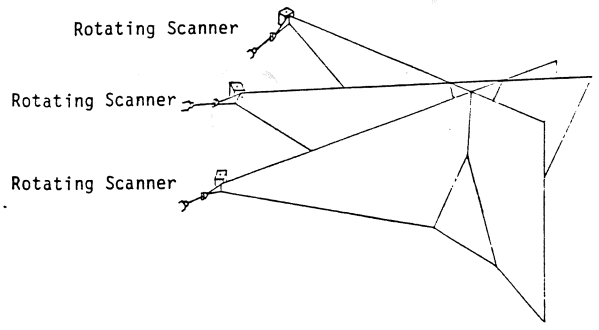

Figure 1: Intersection of Three Planes

INFLUENCE OF PASSIVE ELASTIC JOINT MOMENTS ON HUMAN GAIT

J.M. Mansour and M. Audu
Department of Mechanical and Aerospace Engineering
Case Western Reserve University
Cleveland, OH 44118

INTRODUCTION: The resultant moment at a joint consists of two components: an active component from the contraction of stimulated muscle and a passive component from the deformation of tissues surrounding the joint when the muscles are not stimulated. The total passive moment at a joint is viscoelastic. For this investigation, the elastic contribution to the viscoelastic response was measured.

METHODS: An experimental apparatus was designed to measure the passive elastic moment at the hip as a function of hip and knee angles. All tests were performed with the subject in a side lying position with the trunk fixed. The leg was rotated in the horizontal plane. The force needed to rotate the leg was measured by a load cell mounted distal to the leg. An electrogoniometer measured hip and knee angles.

The hip was exercised through a range from approximately zero degrees to 60 degrees of flexion. Eight fixed knee angles were used ranging from approximately zero degrees to 70 degrees of flexion in 10 degree increments.

RESULTS AND DISCUSSION: Two joint muscles were found to have an anatomically consistent effect on the passive hip moment. With the knee in its maximum flexed position the hip moment was greatest in hip extension and least in hip flexion. This was attributed to the biasing moment induced at the hip due to the stretching of the rectus femoris by flexing the knee. Conversely, with the knee in its extended position the hip moment was greatest in hip flexion and least in hip extension. This was attributed to the biasing moment induced at the hip due to the stretching of the hamstrings by extending the knee.

The passive hip moment takes on potential significance when evaluated relative to the total joint moment in a common activity such as walking. Using typical joint angles for toe off and incipient heel strike, the corresponding passive hip moments for all subjects tested were 10 to 15 N-m at toe off and 20 to 40 N-m at incipient heel strike. The passive hip moment, at toe off, was approximately 30% to 50% of the total hip moment during walking (2). The influence of the passive moment just before heel strike was more difficult to evaluate, as the total moment was changing rapidly at this time. Using maximum and minimum values of the total moment around heel strike the passive hip moment was approximately 60% to 100% of the total moment at this time. An implication of this analysis is the possibility of passive elastic energy storage and release during human gait. Based on these results, an investigation of the influence of the passive elastic component of knee moment was initiated.

Approximations have been introduced in making these evaluations since the moment data for gait was from an independent source. However, the apparently high contribution of the passive joint moment to the total moment does not appear to be insignificant.

ACKNOWLEDGEMENT: This work was supported by the NIH grant #AM 32366.

REFERENCES: 1. Yoon, Y.S. and Mansour, J.M. (1982). The passive elastic moment at the hip, J. Biomech., 15: 905-910.
2. Bresler, B. and Frankel, J.P. (1950). The forces and moments in the leg during level walking, Trans. Am. Soc. Mech. Engr., 72: 27-36.

THE SENSITIVITY OF SKIN TO STRAIN RATE OF LOADING

Roger C. Haut, Ph.D.
General Motors Research Laboratories
Biomedical Science Department
Crash Injury Section
Warren, MI 48090

Abstract

Dynamic tensile strength is an important characteristic of skin commonly associated with the potential for laceration from blunt impact. Skin, like other connective tissue, is a complex composite material of high-modulus collagenous fibrils and low-modulus fibrils of elastin embedded in a hydrated macromolecular matrix of glycosaminoglycans (GAG). The "static" or low strain rate strength of human and animal skin has been correlated with the concentration of collagen in the tissue. However, impact trauma occurs at high strain rate and non-collagen components may play an important role. The constitution of skin is known to vary with the degree of maturation and age. The objective of the current study was to measure the "static" and "dynamic" strength of skin at various ages in an animal model and correlate mechanical and biochemical parameters.

Micro-tensile test specimens (ASTM D-1708) were cut parallel to the spine from dorsal skin flaps of Fischer rats aged 1 to 21 months. Tensile failure experiments were conducted on saline moistened specimens at high (1350 mm/s) and low (6.8 mm/s) speeds with a servo-controlled hydraulic test machine. Specially designed pneumatic grips clamped the specimen avoiding slippage. The sensitivity of the tissue to strain rate was determined by the ratio of dynamic to static mechanical response. Total collagen content was measured as mg hydroxyproline per g dry weight. Tissue GAG was determined by uronic acid concentration.

Quasi-static experiments indicate the tensile strength of dorsal rat skin increased significantly between the ages of 1 and 2 months, and remained constant thereafter. This paralleled change in the concentration of tissue hydroxyproline. Quasi-static failure strain did not significantly depend on age. The sensitivity of tensile strength to strain rate depended on age. The ratio dropped from 2.54 ± 0.51 ($N = 3$) at 1 month to 1.45 ± 0.23 at 6 months, and remained constant thereafter. Age-dependent change in the sensitivity ratio paralleled the content of GAG to collagen in the tissue. Failure strain was independent of strain rate.

Other investigators commonly suggest certain time-dependent mechanical characteristics of connective tissue are, in part, controlled by the matrix of GAG. The current study on dorsal rat skin supports this contention. While the mechanism of GAG interaction with collagen is yet unknown, similar results may be expected in human skin. An earlier study of laceration using aged human skin specimens indicated an increase of 150% in tensile strength over three orders of magnitude increase in loading rate. The current study would suggest an even greater sensitivity of skin to strain rate at young ages, especially during adolescence.

The 20 MHz Pulsed Ultrasonic Doppler Velocity Meter: A Method for Assessing Flow in Small Vessels

William F. Blair
Department of Orthopaedics
University of Iowa
Iowa City, Iowa 52242

Douglas R. Pedersen
Orthopaedic Biomechanics Laboratory
University of Iowa
Iowa City, Iowa 52242

The quantification of blood flow in microsurgical models is a desirable but difficult goal to accomplish. The 20 MHz pulsed ultrasonic Doppler velocity meter (PUDVM) is an instrument which reproducibly and precisely accomplishes the goal, without manipulation of the vessel in study. The instrument has directional, variable range and pulse width capabilities. A single piezoelectric crystal is pulsed with 0.2-5.2 microsecond bursts of energy, at a pulse repetition rate of 62.5 KHz. The axial length of the sample volume is adjustable from lengths of 0.3 mm to 4.0 mm. The center of the sample volume can be positioned 1 to 10 mm from the transducer. The frequency shift in the Doppler audio signal is directly proportional to the velocity of blood cells by the Doppler equation: $V = \frac{\Delta f \cdot C}{2f \cdot \cos\theta}$. Since the first moment of the Doppler audio spectrum is proportional to the average velocity of blood cells, and the sample volume is adjustable, measurements of spatial mean velocity (Vsm), temporal mean of the spatial mean velocity ($\overline{Vsm}$), velocity profiles are available. Velocity profiles permit a calculation of flow stream cross-sectional area. Volumetric blood flow is then calculated ($Q = \overline{Vsm} \cdot A$).

Programming currently allows computerized data collection, storage, and processing of the PUDVM output signal. Recent modifications in method replace electronic filtering of the Vsm with computer averaging to derive $\overline{Vsm}$. Also, our system includes an instrument for programmed, automated flow control advance. Utilizing this data acquisition system in microsurgical models we have described:

1) blood flow in normal 1.0 mm rat femoral arteries, where $\overline{Vsm}$ = 6.1 cm/sec and Q = 3.6 cc/min
2) the influence of topical lidocaine on normal arterial flow, with a 21% increase in $\overline{Vsm}$ and a 35% increase in Q, 3 minutes after application
3) the short term results of microarteriorrhaphy on small vessel flow parameters, with a 30% decrease in $\overline{Vsm}$ and a 50% decrease in Q
4) the effects of topical lidocaine on the microsurgical arteriorrhaphy, with an acceleration of the rate of return of velocities and blood flows to preoperative values.

Most recently we have successfully compared interrupted and continuous suturing techniques in the microarteriorrhaphy of 1.5 mm vessels, demonstrating 13.2 cc/min and 13.1 cc/min postoperative flows in the two study groups, respectively. We propose that 20 MHz PUDVM method will remain a valuable research tool in the microsurgical laboratory.

Aided by a grant from the Orthopaedic Research and Education Foundation, 444 North Michigan Avenue, Suite 1550, Chicago, Illinois, 60611

AUTHOR INDEX

Adrian, M. 30, 42
Allard, P. 40
An, K. N. 13, 29
Anderson, C. K. 5
Andersson, G. 39
Andriacchi, T. P. 35, 37
Arms, S. W. 23
Armstrong, T. J. 1
Audu, M. 47

Behrens, F. 33
Belcher, M. K. 37
Blair, W. F. 49
Brand, R. A. 16
Bridges, M. S. 12
Butler, D. L. 22, 24

Cabanela, M. 32
Carr, D. 20
Carter, D. R. 9
Chaffin, D. B. 25
Chao, E. Y. S. 13, 29, 32
Chilbert, M. 18
Cochran, D. J. 6
Cooney, W. P. 13
Cusick, J. F. 18

Dansereau, J. 40
Davy, D. T. 10
de Lange, A. 15
Dickie, D. L. 12
Donath, M. 36, 38, 46
Donnermeyer, D. 27
Duhaime, M. 40

Eken, M. S. 36
Ewing, C. 18

Flynn, M. J. 12
Fischer, R. A. 23
Freivalds, A. 26
Frymoyer, J. W. 20

Garg, A. 25
Gilbertson, L. 20
Goldstein, S. A. 11, 12
Gomez, M. A. 21

Gray, G. W. 31
Greenapple, D. M. 17
Grood, E. S. 22
Gross, R. M. 29

Hart, R. T. 10
Haut, R. C. 48
Head, J. 43
Hohn, R. B. 22
Huiskes, R. 15
Hult, E. 39
Hwang, I. 42

Jodat, R. 18
Johnson, R. J. 23
Johnson, W. D. 33
Jorneus, L. 39
Joynt, R. L. 7

Kaderly, R. 22
Kaleps, I. 26
Kasman, R. 11, 32
Kazarian, L. E. 19
Keller, D. 27
Keller, T. S. 9
King, A. I. 7
Krag, M. H. 20

Larson, S. J. 18
Linscheid, R. L. 13
Lovin, J. D. 9

Maiman, D. J. 18, 41
Mansour, J. M. 47
Marras, W. S. 7
Martin, R. B. 34
Matthews, L. S. 11
Mattsson, L. 39
MacFarlane, J. 38, 46
Minami, A. 13
Mohan, D. 44
Moskowitz, S. E. 45
Mostardi, R. A. 28
Myklebust, J. B. 18, 41

Newton, P. O. 21
Noyes, F. R. 22

Olmstead, M. L. 22

Panjabi, M. 39
Pedersen, D. R. 16, 49
Pintar, F. 41
Pope, M. H. 20, 23, 27
Porterfield, J. A. 8, 28

Rab, G. T. 14
Raso, J. V. 40
Reider, B. 37
Riley, M. W. 6

Sahay, K. B. 44
Sances, A. 18, 41
Schein, S. S. 35
Shiba, R. 32
Siegel, M. 22
Smith-Lagnese, S. D. 19
Spengler, D. M. 9
Stokes, I. A. F. 17
Stouffer, D. C. 24
Strickland, A. B. 35
Susman, R. L. 3

Thiry, P. S. 40
Thomas, D. J. 18

Urycki, S. 28

Weiss, A. P. C. 11
Wilder, D. 27
Wilson, T. A. 4
Winet, H. 43
Woo, S. L. Y. 21
Wu, T. Y. 43

Yamamoto, H. 30
Yates, G. T. 43
Yeater, R. A. 34

Zahalak, G. I. 2
Zernicke, R. F. 24